Journal Pre-proofs

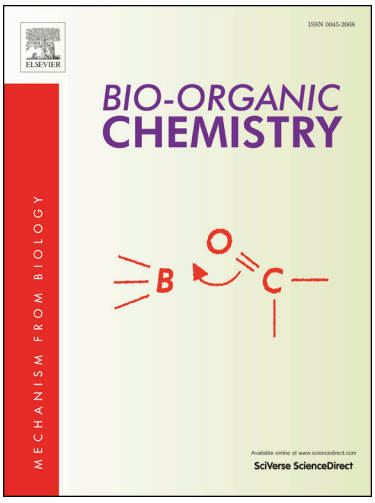

Design and synthesis of new pyranoquinolinone heteroannulated to triazolo-pyrimidine of potential apoptotic antiproliferative activity

Mohamed Ramadan, Mohamed Abd El-Aziz, Yassin A. M. M. Elshaier, Bahaa G.M. Youssif, Alan B. Brown, Hazem M. Fathy, Ashraf A. Aly

PII: S0045-2068(20)31690-4
DOI: https://doi.org/10.1016/j.bioorg.2020.104392
Reference: YBIOO 104392

To appear in: *Bioorganic Chemistry*

Received Date: 30 July 2020
Revised Date: 3 September 2020
Accepted Date: 15 October 2020

Please cite this article as: M. Ramadan, M. Abd El-Aziz, Y. A. M. M. Elshaier, B.G.M. Youssif, A.B. Brown, H.M. Fathy, A.A. Aly, Design and synthesis of new pyranoquinolinone heteroannulated to triazolopyrimidine of potential apoptotic antiproliferative activity, *Bioorganic Chemistry* (2020), doi: https://doi.org/10.1016/j.bioorg.2020.104392

Design and synthesis of new pyranoquinolinone heteroannulated to triazolopyrimidine of potential apoptotic antiproliferative activity

Mohamed Ramadan[a*], Mohamed Abd El-Aziz[b], Yassin A. M. M. Elshaier[c], Bahaa G.M. Youssif[d*], Alan B. Brown[e]; Hazem M. Fathy[a] and Ashraf A. Aly[f*]

[a]Organic Chemistry Department, Faculty of Pharmacy, Al-Azhar University, Assiut Branch,71524 Assuit, Egypt; [b]Medicinal Department, Faculty of Pharmacy, Minia University, 61519 El Minia, Egypt; [c]Organic and Medicinal Chemistry Department, Faculty of Pharmacy, University of Sadat City, 32958 Menoufia, Egypt; [e]Pharmaceutical Organic Chemistry Department, Faculty of Pharmacy, Assiut University, Assiut, 71526, Egypt; [e]Chemistry Department, Florida Institute of Technology, Melbourne, FL 32901, USA; [f]Chemistry Department, Faculty of Science, Minia University, 61519 El-Minia, Egypt

Corresponding Authors: Prof Ashraf A. Aly, e-mail: ashrafaly63@yahoo.com; Dr Mohamed Ramadan, e-mail: elbashamohammed@yahoo.com and Dr Bahaa G.M. Youssif, e-mail: bgyoussif@ju.edu.eg.

Abstract

Pyrano[3,2-*c*]quinoline derivatives have been synthesized and utilized to obtain various new hetero-annulated triazolopyrimidine, containing quinoline, pyran, 1,2,4-triazine and pyrimidine in good yields. Newly synthesized compounds have been characterized by spectral data and elemental analysis. Most of the synthesized compounds showed moderate to weak antiproliferative activity on most cancer cell lines, especially leukemia and breast cancer cell lines. The open chain formimidic acid ethyl ester is slightly more potent than hetero-annulated systems. The most active compounds were further investigated for caspase activation, Bax activation and Bcl-2 down regulation compared to doxorubicin as a standard, and indeed exhibited mainly cell cycle arrest at the Pre-G1 and G2/M phases. The transcription effects of **5a** and **5b** on the p53 were assessed and compared with the reference doxorubicin. The results revealed an increase of 12-19 in p53 level compared to the test cells and that p53 protein level of **5a** and **5b** was significantly inductive (991, and 639 pg / mL, respectively) in relation to doxorubicin (1263 pg / mL)

Keywords: Pyrano[3,2-*c*]quinoline, triazolopyrimidine, formimidic acid , caspase, apoptosis, antiproliferative.

Highlights

- A series of pyrano[3,2-c]quinoline/triazolopyrimidine hybrids was made.
- Products were characterized by IR, MS, and multinuclear NMR (^{1}H, ^{13}C, and ^{15}N).
- The products showed antiproliferative activity versus cancer cell lines.
- Open chain formimidic esters were more potent than heteroannulated systems.
- The most active compounds were also studied for caspase activation.
- Compounds **5a** and **5b** showed an increase of 12-19 in p53 level compared to the test cells.
- The drug likeness profile of the synthesized compounds was predicted using the Swiss ADME website.

1. INTRODUCTION

Nitrogen containing heterocyclic compounds is a notable form of anticancer drug applicant that strongly promotes cell apoptosis [1]. Many quinoline containing compounds have been reported as potential antitumor agents [2,3]. Quinoline skeletal perform an important aspect in anticancer drug improvement, as their derivatives show great results through different operations such as growth inhibitors by cell cycle arrest, apoptosis, inhibition of angiogenesis, disruption of cell migration, and modulation of nuclear receptor responsiveness [4]. The fused pyranoquinoline moiety is an extremely common structural motif that occurs in many naturally occurring or biologically active alkaloids, such as flindersine, atanine, tabouensinium chloride, zanthoxylum simulans, oricine, verprisine, and araliopsis tabouensis [5-7]. The unique biological activity of the pyranoquinoline derivatives has made these compounds privileged targets in recent medicinal studies. For instance, compounds that contain a pyranoquinoline nucleus have been frequently used for bactericidal and bacteriolytic activities [8,9], acetylcholinesterase inhibition [10], antiallergenic [11], anti-inflammatory [12], antimalarial [13], calcium-signalling inhibition [14], platelet aggregation [6] and antitumor activities [15-18]. Recently, a pyranoquinoline nucleus has been employed in the pharmacophores with potential medicinal features against various diseases, like Alzheimer's [19], venereal [5] and psychotropic [20].

The triazolo-pyrimidine moiety has been extensively used as a template in medicinal chemistry for its diverse pharmacological properties. Due to its ability to bind to a wide range of enzymes and receptors through various non-covalent interactions, triazolo-pyrimidines have been extensively investigated and are known to have a versatile biological potential [22]. A series of triazolopyrimidine derivatives have been found to be potentially useful as cyclin-dependent kinase inhibitors [23] and have also shown antiproliferative activity on the cancer cell line [24]. Moreover, some triazolo-pyrimidines were reported to enhance the antitumor activity [25]. The

significance of the triazolo-pyrimidine moiety in the cytotoxic activity of certain derivatives [26] and their incorporation into many complex systems has been reported [21], in addition, these derivatives proved to be active as anticancer agents [27]. In addition, triazolo-pyrimidine derivatives were also found to induce apoptosis and/or reduce cell proliferation in different solid tumors and several human cancer cell lines [28]. We reported the synthesis of ethyl 5,6-dihydro-2,5-dioxo-6,9-disubstituted-2*H*-pyrano[3,2-*c*]quinoline-4-carboxylates **I**, **Figure 1** from the reaction of equimolar amounts of 2,4(1*H*,3*H*)-quinolinediones and diethyl acetylene dicarboxylate in absolute ethanol, containing catalytic triethylamine [29]. In previous work with quinolones, *Aly et al*. synthesized various classes of 2-quinolones such as 2'-amino-2,5'-dioxo-5',6'-dihydro-spiro(indoline-3,4'-pyrano[3,2-*c*]quinoline)-3'-carbonitriles **II** [30], 3-(methylthio)-4-oxo-4,5-dihydrofuro[3,2-c]quinolone-2-carbonitriles **III** [31], naphtho[2',3':4,5]furo[3,2-c]quinoline-6,7,12(5*H*)-trione derivatives **IV** (as ERK inhibitors with efficacy in BRAF-mutant melanoma) [32], 2,3-bis-(4-hydroxy-2-oxo-1,2-dihydroquinolin-3-yl)succinates, and arylmethylene-bis-3,3'-quinoline-2-ones **V** [33], and *N*-2,3-bis(6-substituted-4-hydroxy-2-oxo-1,2-dihydroquinolin-3-yl)naphthalene-1,4-diones **VI** [34] , **Figure 1**.

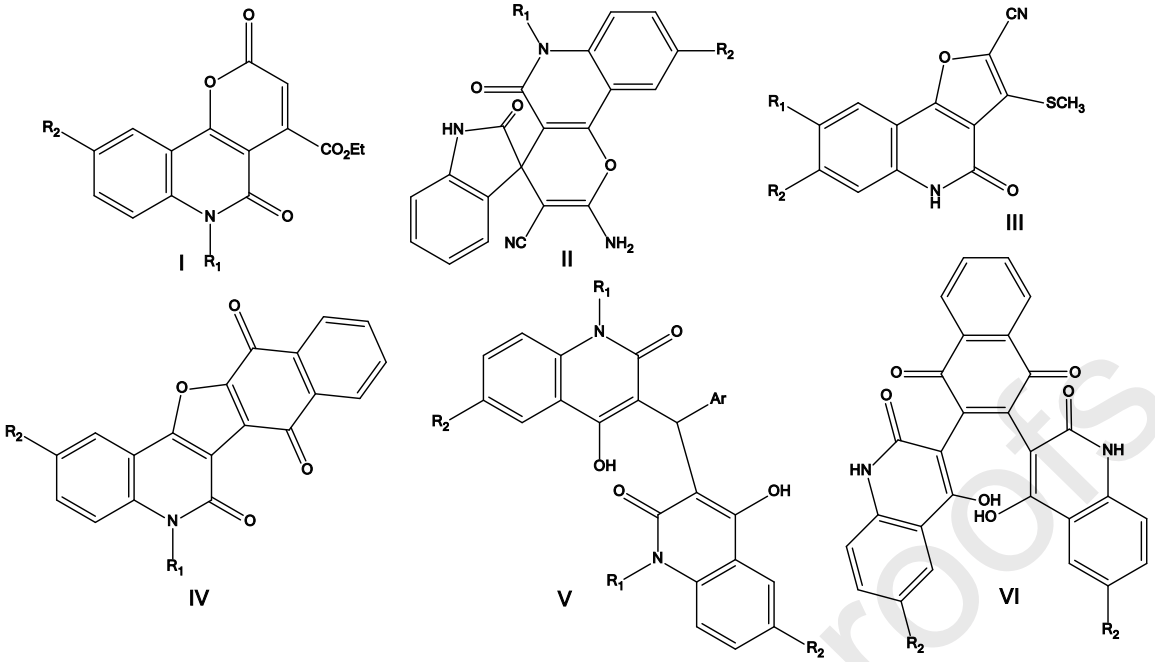

Figure 1. Chemical structure of some previously reported Quinolones **I-VI**

In view of the important properties described above, the synthesis of heterocyclic molecules containing these nuclei has become increasingly important in organic synthesis. Encouraged by their potential clinical applications and in continuation of our work on bio-potent heterocycles, our efforts are focused to design and synthesize newer biologically potent heterocyclic systems *via* combination of the two therapeutically active moieties pyranoquinoline and triazolopyrimidine together in a single scaffold. The cytotoxic activity of the synthesized compounds against the NCI-60 cancer cell line panel was determined and the most effective inhibitors were further investigated for Caspases 3, 8, 9 and Cytochrome C, as well as the enzymatic activity on p53 as a possible plausible mechanism for their anticancer efficacy.

2. Results and discussion

2.1.Chemistry

Synthesis of compounds **5a-e, 8a-e,** and **9a-e** was illustrated in **Scheme 1**. Equimolar amounts of 1,6-disubstituted quinoline-2,4-(1*H*,3*H*)-diones **1a-e** and 2-(4-chlorobenzylidene) malonitrile **2** refluxed in absolute ethanol containing piperidine as a basic catalyst, provided the pyranoquinoline derivatives **3a-e** as yellow powders in excellent yields. Elemental analysis and spectral data agreed well with the assigned structures **3a-e** (**Scheme 1**).

The IR spectrum of compound **3c,** for example, showed characteristic absorption bands at ν_{max} = 3387, and 2234 cm^{-1} corresponding to the NH_2 and the C≡N groups, respectively. The ^1H NMR spectrum of compound **3c** displayed a characteristic singlet at δ_H 7.30 assigned to NH_2-pyran and two singlets at δ_H 2.39 and 4.51 assigned to methyl group and CH-pyran, respectively. The ^{13}C NMR spectrum of **3c** showed a characteristic signal at δ_C 191.61 assigned to C-CN and two carbon signals in the aliphatic region at δ_C 57.30 and 36.24 assigned to C-3 and C-4 of the pyran ring, respectively. The mass spectra and elemental analyses indicated that the molecular weight is consistent with the molecular formula of the target compounds.

Subsequent treatment of **3a-e** with an excess of orthoformic esters **4a**,**b** in the presence of acetic anhydride afforded the desired formimidic acid esters **5a-e**. The assignment of the structures of **5a-e** was established based on their spectral data (IR, ^1H NMR, ^{13}C NMR and MS) and elemental analyses. For example, the IR spectrum of compound **5c** showed disappearance of the characteristic band of NH_2 and appearance of absorption bands at ν_{maz} = 3154, 2243 cm^{-1} characteristic of C=H and C≡N, respectively. The ^1H NMR spectrum revealed absence of singlet at δ_H 7.30 characteristic of NH_2-pyran and appearance of distinctive three sets of alkene and ethoxy signals at δ_H 8.94, 4.37 and 1.34 corresponding to

H-2b, H-2d and H-2e, respectively; the attached carbons appear at δ_C 159.65, 63.48 and 13.34 for C-2b, C-2d and C-2e, respectively, which confirmed the nucleophilic attack of the lone pair of electrons of pyran-NH_2 on orthoformic ester.

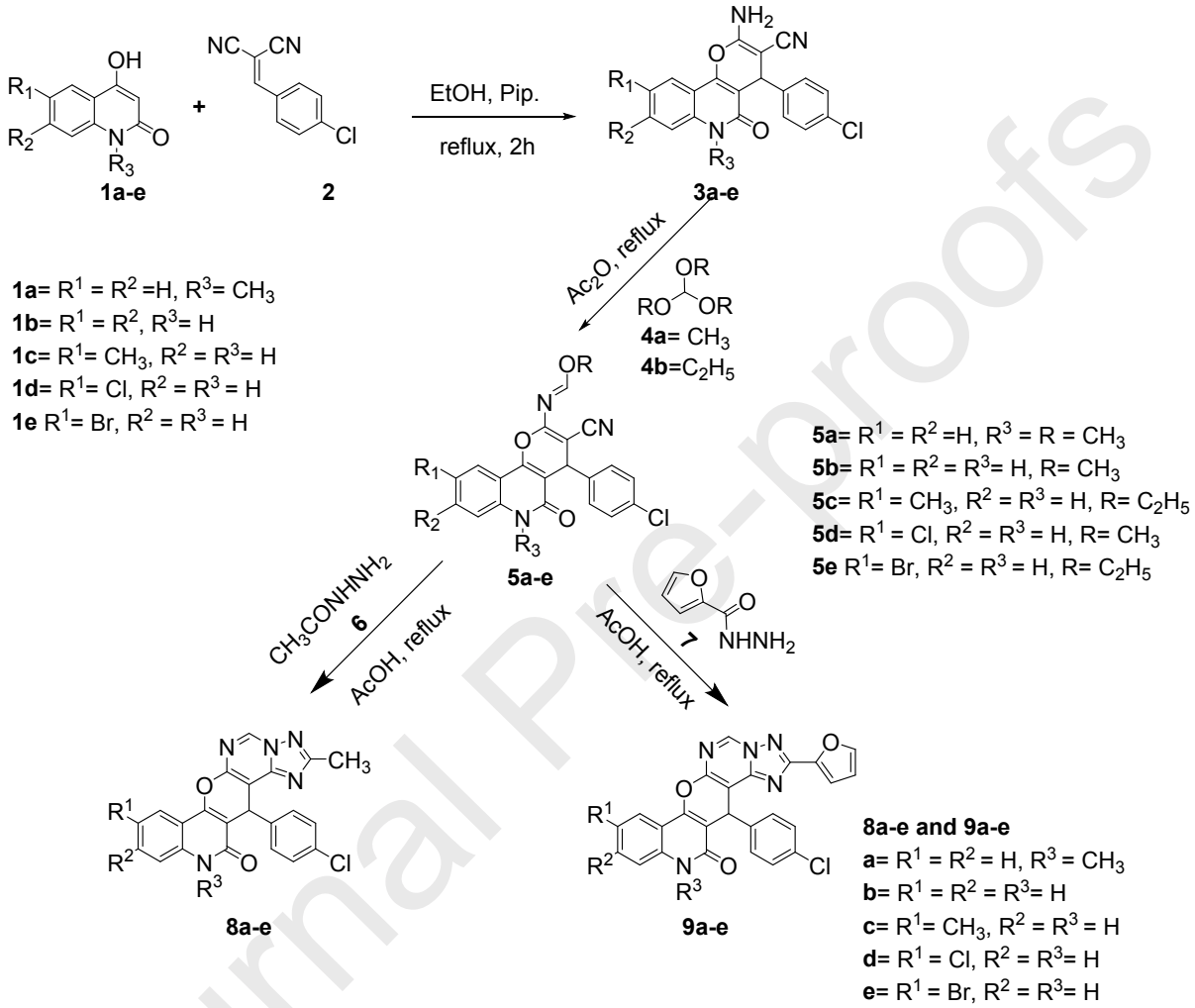

Scheme 1. Synthesis of the compounds **5a-e, 8a-e,** and **9a-e**.

The reaction mechanism presumably starts by proton abstraction by piperidine then Michael addition and intramolecular cyclization, isomerization, followed by nucleophilic attack of the lone pair of electrons of pyran-NH_2 on orthoformic ester **4** to afford the corresponding products **5a-e** (**Scheme 2**).

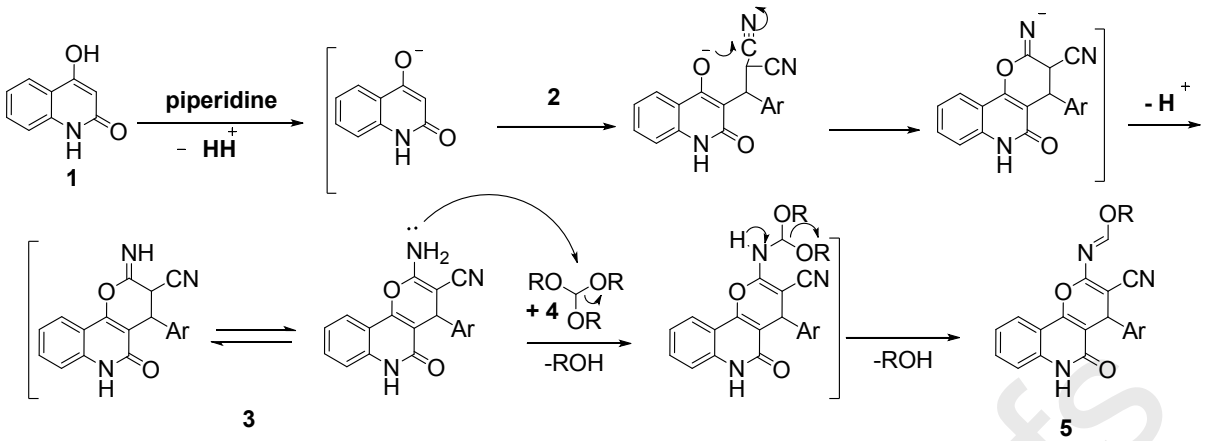

Scheme 2. Suggested mechanism for the formation of compounds **3a-e** and **5a-e**.

The new compounds **5a-e** could enter cascade heterocyclization with acetohydrazide **6** or furan-2-carbohydrazide **7** to form triazolopyrimidine hybrids **8a-e** and **9a-e** respectively, as shown in **Scheme 1**. The cyclization was established by recording its IR, NMR and MS spectra. As a representative example for series **8a-e**, the IR spectrum of **8a** showed the absence of nitrile and carbonyl groups; this gives a strong indication of cyclization of **5a** to form **8a**. Also, the ^{1}H NMR spectrum of compounds **8c** and **9c** showed the absence of ethoxy signals at δ_H 4.37 and 1.35 for H-2d and H-2e, respectively. In addition, they showed singlet signals at δ_H 10.08 and 10.14 integrating for one proton of pyrimidine ring of compound **8c** and **9c**, respectively. The smooth cyclization of **8a** was further confirmed by characteristic ^{13}C NMR signals at δ_C 161.75 (C-2), 149.73 (C-14b), 144.02 (C-5), and 104.61 (C-14a). Additionally, all five nitrogens can be observed: N-12 gives HMBC correlation with H-11, N-1 and N-3 correlate with H-2a. N-4 and N-6 correlate with H-5. N-1 is differentiated from N-3, and N-4 from N-6, based on hybridization. On the other hand, the ^{1}H NMR spectrum of **9c** showed three singlets at δ_H 8.22, 8.05 and 7.19 corresponding to the furan ring protons H-2d, H-2b, and H-2c respectively, and showed only three nitrogens, two of which correlate with H-5. Finally, the structure of the compound **8c** and **9c** was confirmed by their mass spectra, which showed molecular ion peaks at *m/z* = 429 and 481 which are consistent with the molecular formula $C_{23}H_{16}ClN_5O_2$ and $C_{26}H_{16}ClN_5O_3$, respectively (**Table 1**).

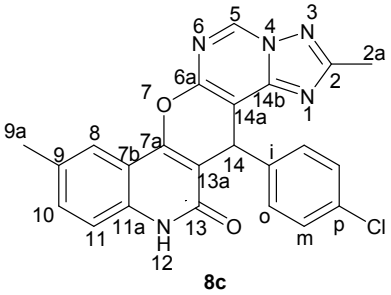

8c

Table 1. NMR spectroscopic assignments of compound **8c**

^{1}HNMR (DMSO-d_6)	**COSY**	**Assignment**
12.05 (s; 1H)		NH-12
10.08 (bs; 1H)		H-5
8.73 (d, *J* = 1.6; 1H)	*8.24, 3.09*	H-8
8.24 (d, *J* = 8.2; 1H)	*8.73,* 8.07	H-10
8.07 (d, *J* = 8.5; 1H)	8.24	H-11
7.85 (d, *J* = 7.9; 2H)	7.74	H-m
7.74 (d, *J* = 7.8; 2H)	7.85	H-o
6.44 (s; 1H)		H-14
3.22 (s; 3H)		H-2a
3.09 (s; 3H)	*8.73*	H-9a

^{13}C NMR (DMSO-d_6)	**HSQC:**	**HMBC:**	**Assignment**
164.0		6.38, 4.33	C-13
161.75		3.22	C-2
160.49		10.08, 6.44	C-6a
158.17		8.73, *8.07, 6.44*	C-7a
149.73		10.08	C-14b
144.02	10.08	10.08	C-5
141.11		8.07, 3.09	C-9
138.72	8.24	8.73, 7.85, 7.74	C-10
138.58		8.73, 7.74	C-*i*
137.58		8.73, 7.74	C-*p*
136.72		8.73, 8.24, *6.44*	C-11a
132.04	7.85	7.85, 6.44	C-*m*
131.88	7.74	7.74, 6.44	C-*o*
123.96	8.73	8.24,3.09	C-8
119.47	8.07		C-11
116.26		8.07	C-7b
107.17		6.44	C-13a
104.61		10.08, 6.44	C-14a
37.39	6.44	7.85	C-14
21.90	3.09	8.73, 8.24, 3.09	C-9a
12.59	3.22	3.22	C-2a

^{15}NNMR (DMSO-d_6)	**HSQC**	**HMBC:**	**Assignment**
263.5		3.22	N-3
243.9		10.08	N-6
226.0		10.08	N-4
149.6		3.22	N-1
147.4		8.07	N-12

The heterocyclization starts by nucleophilic attack of the hydrazide amino lone pair of electrons of compounds **6** and **7** on the imine carbon of **5** with elimination of a molecule of alcohol, followed by a second nucleophilic attack on the nitrile carbon, then intramolecular cyclization of imine lone pair on carbonyl carbon with extrusion of a water molecule to afford compounds **8a-e** and **9a-e** (**Scheme 3**).

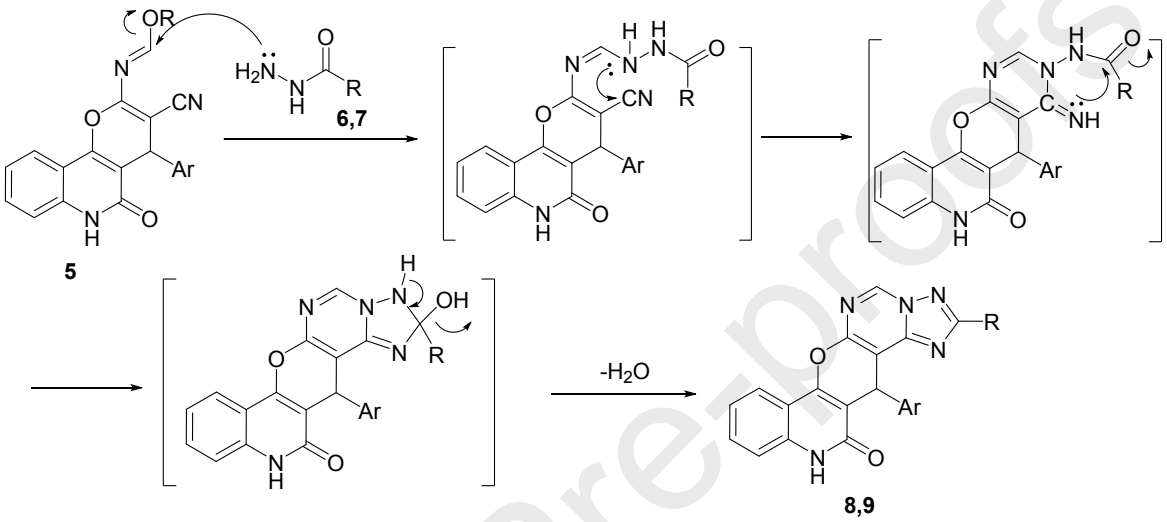

Scheme 3. Plausible mechanism for the formation of compounds **8a-e** and **9a-e**.

2.2. Evaluation of biological activities

2.2.1. Screening of antiproliferative activity by NCI

The target compounds **5a-e, 8a-e** and **9a-e** were selected by the National Cancer Institute [NCI, Bethesda, MD, USA (http://www.dtp.nci.nih.gov.)] for evaluation at a single concentration of 10 μM towards a panel of sixty cancer cell lines of nine diverse tissues according to NCI protocol [35, 36]. The screening results were reported as the percent growth inhibition of treated cells compared to untreated control cells. Results in **Table 2** revealed that most compounds showed weak to moderate activities on most cell lines especially, leukemia and breast cancer cell lines. Moreover, the results revealed that**,** the open chain formimidic acid ethyl ester **5a-e** exhibited variable degrees of growth inhibitory activity towards a majority of the tested cancer cell lines than the cyclized triazolo-pyrimidine derivatives **8a-e** and **9a-e**. Additionally, it is

obvious that the electronic effect on both position of substituent on the tested scaffolds had a pronounced effect on their cytotoxic activity. Compound **5a** with quinoline N-methyl (electron donating group) showed more antiproliferative activity on a majority tested leukemia and breast cancer cell lines than compounds **5b** and **5d** with unsubstituted or electron withdrawing group respectively (**Table 2**). Compound **5a** showed promising activities against SR, K-562, MDA-MB-468, MDA-MB and MCF7 achieving 77.26, 80.38, 46.02, 48.75 and 58.30 % of growth inhibition respectively; However, compound **5b** and **5d** showed weak cytotoxic activities against the same cell lines. On the other hand, triazole-2-methyl derivatives **8a-e** and triazole-2-furan **9a-e** were less potent than the open chain derivatives **5a-e**. Exceptionally, compound **8a** showed moderate antiproliferative activity against RPMI-8226 and HOP-92 achieving 48.89 and 48.91% of growth inhibition respectively.

Table 2: Percentage growth inhibition (GI %) of *in vitro* subpanel tumor cell lines at 10 μM concentration for compounds **5a-e**, **8a-e**, and **9a-e**.

Subpanel cancer cell Lines	% Growth Inhibition (GI %) [a]														
	5a	**5b**	**5c**	**5d**	**5e**	**8a**	**8b**	**8c**	**8d**	**8e**	**9a**	**9b**	**9c**	**9d**	**9e**
Leukemia															
CCRF-CEM	33.12	26.12	15.24	15.95	12.74	23.80	-	-	-	-	-	-	13.45	-	-
HL-60(TB)	46.57	27.34	18.27	18.31	11.36	33.79	-	17.70	-	-	10.10	-	13.65	-	-
K-562	**80.38**	20.04	22.10	19.25	11.90	21.50	-	15.64	-	-	8.44	-	11.07	-	-
MOLT-4	24.81	11.92	-	11.30	-	24.14	-	-	-	-	-	-	-	-	-
RPMI-8226	11.90	41.62	35.12	33.79	69.81	48.89	13.79	30.74	-	-	-	-	-	-	13.89
SR	**77.26**	37.74	19.07	25.22	13.32	16.65	-	-	-	-	-	-	31.47	-	-
Non-small cell lung cancer															
A549/ATCC	36.35	25.15	10.05	-	-	13.62	-	-	-	-	-	-	-	-	-
EKVX	26.02	51.18	18.04	18.32	30.46	22.72	13.90	21.29	11.84	-	9.01	-	14.54	-	-
HOP-62	35.37	50.04	25.26	19.40	29.26	15.39	12.72	13.67	-	-	2.21	-	-	-	-
HOP-92	20.83	62.30	38.58	38.91	49.25	48.91	25.85	34.83	-	-	12.06	21.53	29.77	-	31.91
NCI-H226	-	34.54	15.58	18.36	21.07	13.11	-	-	-	-	-	-	-	-	-
NCI-H23	19.67	23.92	13.70	12.90	14.63	-	-	-	-	-	-	-	-	-	-
NCI-H322M	14.08	24.70	-	-	12.01	-	-	-	-	-	-	-	-	-	-
NCI-H460	20.12	14.92	-	-	-	-	-	-	-	-	-	-	-	-	-

NCI-H522	41.29	30.65	27.90	21.49	25.84	24.06	12.40	16.94	-	-	-	-	16.00	24.84	-
Colon cancer															
COLO 205	-	-	-	-	-	12.36	-	-	-	-	-	-	-	-	-
HCC-2998	-	13.44	-	-	-	-	-	-	-	-	-	-	-	-	-
HCT-116	18.35	32.49	11.18	-	17.59	16.05	11.18	15.12	-	-	11.12	-	-	-	-
HCT-15	16.13	35.05	-	-	-	14.16	-	-	-	-	-	-	-	-	-
HT29	25.49	27.02	-	-	19.50	13.66	-	-	-	-	-	-	-	-	-
KM12	-	-	-	-	-	-	-	-	-	-	-	-	-	-	-
SW-620	16.61	26.37	-	-	15.40	-	-	-	-	-	-	-	-	-	-
CNS cancer															
SF-268	20.19	25.67	14.31	-	-	16.67	14.31	15..06	-	11.6	-	-	11.68	-	-
SF-295	23.11	12.07	-	-	-	-	-	-	-	-	-	-	-	-	-
SF-539	13.62	34.54	-	-	24.08	16.41	-	13.43	-	-	-	-	-	-	-
SNB-19	13.62	24.20	-	11.79	15.26	20.47	-	22.73	-	13.5	-	-	13.58	-	-
U251	12.61	19.18	-	-	-	18.06	-	-	-	-	-	-	-	-	-
Melanoma															
LOX IMVI	12.60	23.26	-	-	13.17	-	-	11.02	-	-	-	-	-	-	-
MALME-3	14.18	22.51	-	-	18.24	16.08	-	12.02	-	-	-	-	-	-	-
M14	-	25.06	-	-	12.90	-	-	-	-	-	-	-	-	-	-
MDA-MB-435	-	14.84	-	-	-	-	-	-	-	-	-	-	-	-	-
SK-MEL-2	-	10.92	-	-	-	-	-	-	-	-	-	-	-	-	-
SK-MEL-28	-	-	-	-	-	-	-	-	-	-	-	-	-	-	-
SK-MEL-5	11.56	32.63	-	-	12.85	14.78	-	-	-	-	-	-	-	-	-
UACC-257	-	-	-	-	-	-	-	-	-	-	-	-	-	-	-
UACC-62	26.81	40.22	-	-	53.55	-	-	29.66	24.88	-	-	-	-	-	-
Ovarian cancer															
IGROV1	26.57	55.97	-	-	40.94	-	-	18.44	26.18	-	11.27	-	-	-	-
OVCAR-3	-	18.31	-	-	35.75	-	-	-	-	-	-	-	-	-	-
OVCAR-4	24.74	32.47	-	-	31.36	-	-	28.24	20.09	-	2.43	-	16.17	-	-
OVCAR-5	12.54	26.40	-	-	14.85	-	-	-	11.15	-	-	-	13.17	-	-
OVCAR-8	-	20.69	-	-	13.69	-	-	-	-	-	3.12	-	-	-	-
NCI/ADR-RES	-	11.79	-	-	42.71	-	-	14.80	-	-	-	-	-	-	-
SK-OV-3	-	40.16	-	19.52	18.22	-	-	-	11.48	-	-	-	-	-	-
Renal cancer															
A498	34.06	40.39	-	-	52.06	-	-	13.54	44.14	-	-	-	-	-	-
ACHN	13.66	34.57	-	-	24.27	-	-	12.36	14.70	-	-	-	-	-	-
CAKI-1	41.76	53.67	16.16	-	100.28	-	16.16	25.90	30.78	-	42.23	-	24.51	-	-
RXF 393	25.39	40.89	-	-	43.17	-	-	26.55	12.64	-	-	-	-	-	-
SN12C	16.72	25.37	-	-	25.37	-	-	19.90	20.64	-	22.14	-	-	-	-
TK-10	-	-	-	-	-	-	-	-	-	-	-	-	-	-	-
UO-31	36.13	65	35.49	15.14	45.81	20.92	35.49	37.11	39.27	-	33.15	15.14	-	-	-
Prostate cancer															
PC-3	13.77	27.89	16.64	-	42.25	-	16.64	24.23	15.16	-	16.84	-	11.79	-	-

DU-145	-	-	-	-	-	-	-	-	-	-	-	-	-	-	-
Breast cancer															
MCF7	58.30	31.29	-	13.34	8.01	-	-	15.74	19.74	-	13.23	15.38	-	-	-
MDA-MB-231/ATCC	48.75	51.24	12.11	-	21.69	-	12.11	28.67	29.26	-	22.45	-	17.61	-	-
HS 578T	34.77	**64.39**	-	-	2.87	-	-	-	34	-	-	-	-	-	-
BT-549	18.64	23.12	152.73	-	4.72	-	152.73	-	15.06	-	14.23	-	-	-	11.83
T-47D	34.91	39.11	13.97	-	10.40	-	13.97	24.47	26.35	-	15.22	10.76	-	-	-
MDA-MB-468	46.02	14.08	-	-	3.08	-	-	-	-	-	-	-	-	-	-

(–): Weak activity GI <10%.

2.2.2. In vitro anticancer activity

2.2.2.1. Cell viability assay

Cell viability assay was carried out using human mammary gland epithelial cell line (MCF-10A). MCF-10A cells were incubated with compounds **5a-e**, **8a-e**, and **9a-e** for 4 days and 3-(4,5-dimethylthiazol-2-yl)-2,5-diphenyltetrazolium bromide (MTT) assay was used to assess cell viability [37, 38]. There were no cytotoxic effects in all compounds, and for most tested compounds, more than 85% cell viability was reported at 50 μM.

2.2.2.2. Cytotoxic activity evaluation of IC_{50}

The tested compounds **5a-e**, **8a-e**, and **9a-e** were evaluated for their antiproliferative activities against four human cancer cell lines including pancreas cancer cell line (Panc-1), breast cancer cell line (MCF-7), colon cancer cell line (HT-29) and epithelial cancer cell line (A-549) using MTT assay [39, 40] and doxorubicin has been used as the reference compound. Graph Pad Prism software (Graph Pad Software, San Diego, CA, USA) has been used to measure the median inhibition concentration (IC_{50}) for all compounds. Results were illustrated in **Table 3**.

Triazole-2-mehyl derivatives (**8a-e**) and triazole-2-furan **(9a-e)** showed weak to moderate antiproliferative activity with IC_{50} ranging from 16.60 to 32.70 compared to doxorubicin IC_{50} = 1.13μM, **Table 3**. Generally, formimidic acid ethyl ester **5a-e** showed superior antiproliferative activity compared to their triazolo-pyrimidine counterparts (**8a-e**) and **(9a-e)**,

Table 3. For example, the unsubstituted formimidic acid ethyl ester derivative **5b** showed an average IC_{50} of 4.57 μM against the tested cell lines in comparison to triazole-2-methyl derivative **8b** or triazole-2-furan derivative **9b** which showed average IC_{50} = 19.27 and 22.47 μM, respectively. The electronic effect of the substituents appeared in **5a-e** derivatives, electron withdrawing group Cl and Br in compounds **5d** and **5e**, respectively are much weaker than unsubstituted or electron donating group in **5b** and **5a**, respectively. Moreover, the position of the electron donating is important when we compare **5a** and **5c**, introduction of electron donating group to quinoline nitrogen increase activity dramatically. The Formimidic acid ethyl ester **5a** (R_1, R_2 = H, R_3 = CH_3) was the most potent among the synthesized derivatives, with average IC_{50} value 2.85 μM against the four cell lines compared to the reference doxorubicin (IC_{50} = 1.13 μM). (**Table 3**)

Table 3. Antiproliferative activity of compounds **5a-e, 8a-e** and **9a-e** and **Doxorubicin**

Comp.	Cell viability %	Antiproliferative activity IC_{50}± SEM (μM)				
		A-549	MCF-7	Panc-1	HT-29	Average (IC_{50})
5a	**91**	2.9±0.5	2.2±0.08	3.1±0.2	3.2±0.2	2.850
5b	**84**	4.7±0.4	4.3±0.8	4.6±0.6	4.7±0.4	4.575
5c	**86**	7.7±0.4	7.9±0.6	7.6±0.8	7.9±0.8	7.775
5d	**89**	10.9±0.8	10.5±1.1	10.6±0.8	10.4±1.2	10.60
5e	**85**	8.8±3.2	8.5±2.7	8.7±3.1	8.2±3.4	8.300
8a	**87**	30.4±3.2	30.5±2.7	30.7±3.1	31.2±3.4	30.700
8b	**82**	19.2±1.5	18.9±1.2	19.2±2.2	19.8±2.4	19.275
8c	**90**	15.7±2.5	15.6±2.9	15.8±1.9	15.8±1.6	15.725
8d	**90**	16.9±0.3	16.8±1.6	16.6±1.5	16.9±1.1	16.800
8e	**79**	32.5±0.2	32.1±0.1	32.4±0.2	32.9±0.6	32.474
9a	**92**	24.5±2.6	23.6±2.2	24.6±2.9	24.8±1.4	24.375
9b	**96**	22.3±2.5	22.9±1.8	22.5±2.3	22.2±1.4	22.475
9c	**89**	18.2±0.6	17.9±0.3	18.8±0.5	18.9±0.8	18.475
9d	**91**	29.4±3.6	28.5±2.8	32.6±3.5	29.2±8.2	29.925
9e	**89**	25.5±2.6	25.6±2.2	25.6±2.9	25.8±1.4	25.375
Doxorubicin	--	1.21 ± 0.80	0.90± 0.62	1.41 ± 0.58	1.01 ± 0.82	1.136

2.2.3. Activation of proteolytic caspases cascade

Caspase activation plays a crucial role in the initiation and effecting of the apoptotic process [41]. Among the caspases, caspase-3 is a chief player that cleaves multiple proteins in the cells, causing apoptotic cell death [42]. Compounds **5a-c** have been tested for caspase 3 activation and compared with doxorubicin. The results revealed that compounds **5a-c** showed an improvement in caspase 3 levels by 4.7-5.9 fold compared with untreated control cells, and that **5a** was the most active compound with a remarkable over expression of caspase-3 level (388.58 ± 4.20 pg/mL) compared to doxorubicin (503.2 ± 4.22 pg/mL) (**Figure 2**).

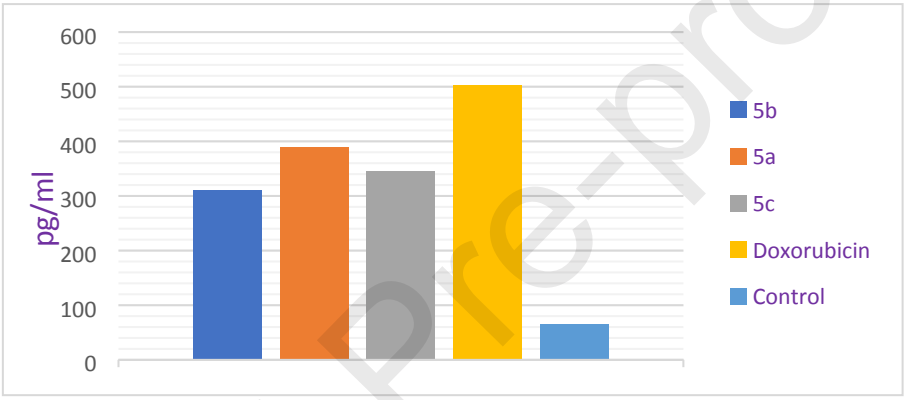

Figure 2. Caspase-3 level for compounds **5a-c** and **doxorubicin** in human breast cancer cell line (MCF-7)

Compound **5a** was further investigated for activation of caspases 8 and caspases 9 and cytochrome C to evaluate the effect of **5a** on the intrinsic and extrinsic apoptotic pathway. It was found that **5a** increases the caspase levels 8 and 9 respectively by 5.47 and 13.79 fold, relative to control cells, which suggests that intrinsic and extrinsic pathways are triggered with greater effect on the intrinsic pathway as caspase 9 levels were higher [43] (**Table 4**).

Table 4. Effects of compounds **5a-c** and doxorubicin on active Caspases 3, 8, 9 and Cytochrome C in MCF-7 breast cancer cell line.

Compound Number	Caspase-3		Caspase-8		Caspase-9		Cytochrome C	
	Conc (pg/ml)	Fold change	Conc (ng/ml)	Fold change	Conc (ng/ml)	Fold change	Conc (ng/ml)	Fold change
5a	388.58 ±4.20	5.92	0.93	5.47	12.83	13.79	0.548	11.91
5b	310.47 ±2.19	4.73	--	--	--	--	--	--
5c	345.92 ±3.92	5.27	--	--	--	--	--	--
Doxorubicin	503.20 ±4.22	7.66	1.75	10.07	16.23	17.40	0.604	13.13
Control	65.64	1	0.17	1	0.93	1	0.046	1

2.2.4. Bax and Bcl-2 levels assay

Compounds **5a** and **5b** were further investigated for their effect on Bax and Bcl-2 levels using doxorubicin as a guide against breast cancer cell line (MCF-7). The results show that compounds **5a** and **5b** increased the Bax level by 29.21 and 20.84-fold greater than the control, compared to doxorubicin 33.43-fold (**Table 5**). In addition, compounds **5a** and **5d** caused a down-regulation of Bcl-2 protein level up to 4.68 and 2.61-fold less than the control compared to doxorubicin 5.17-fold (**Table 5**).

Table 5. Bax and Bcl-2 levels for compounds **5a**, **5b** and Doxorubicin in MCF-7 breast cancer cell line

Compound Number	Bax		Bcl-2	
	Conc (pg/ml)	Fold change	Conc (ng/ml)	Fold change
5a	241.30	29.21	1.085	4.68
5b	172.14	20.84	1.943	2.61
Doxorubicin	276.19	33.43	0.983	5.17
Cont.	8.26	1	5.086	1.00

2.2.5. Flow cytometric cell cycle analysis

Cell cycle analysis was performed in MCF-7 human breast cancer cell line treated with the most active compound **5a**.The percentage of cells in G0/G1 phase of the control was 53.71% which reported a notable decrease to 34.71% upon treatment with compound **5a** while the

percentage of cells in the S phase were slightly reduced with compound **5a** (31.35%) compared to the control (37.42%) (**Figures 3)**. The percentage of MCF-7 human breast cancer cell line at the G2/M phase was apparently increased to 32.14% upon treatment with **5a** compared to the control (8.87%). Moreover, it was observed that the apoptotic cell percentage in the Pre-G1 phase was increased from 1.93% for control untreated cell to 21.34% and 22.17% in cells treated with **5a** and doxorubicin, respectively (**Figures 3** and **4**). According to the above results, compound **5a** exhibited mainly cell cycle arrest at the Pre-G1 and G2/M phases. In addition, the compound studied is not cytotoxic but antiproliferative which induces programmed cell death and cell cycle arrest.

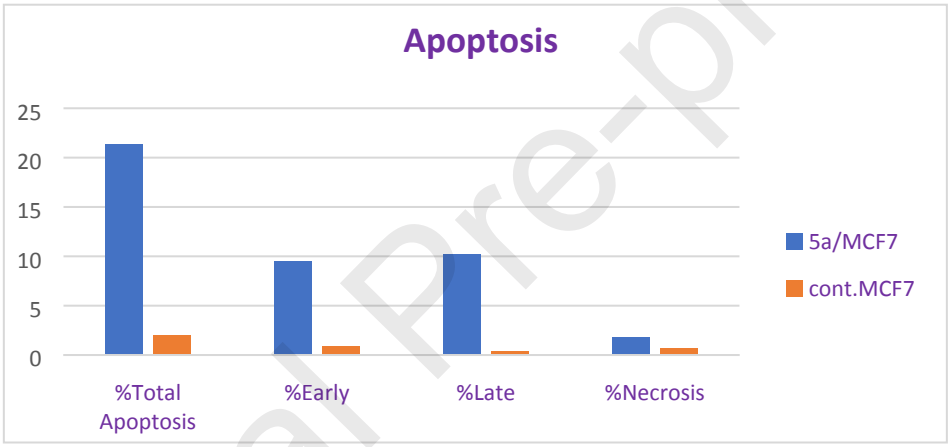

Figure 3. Apoptosis induction analysis using Annexin V/PI for compound **5a**

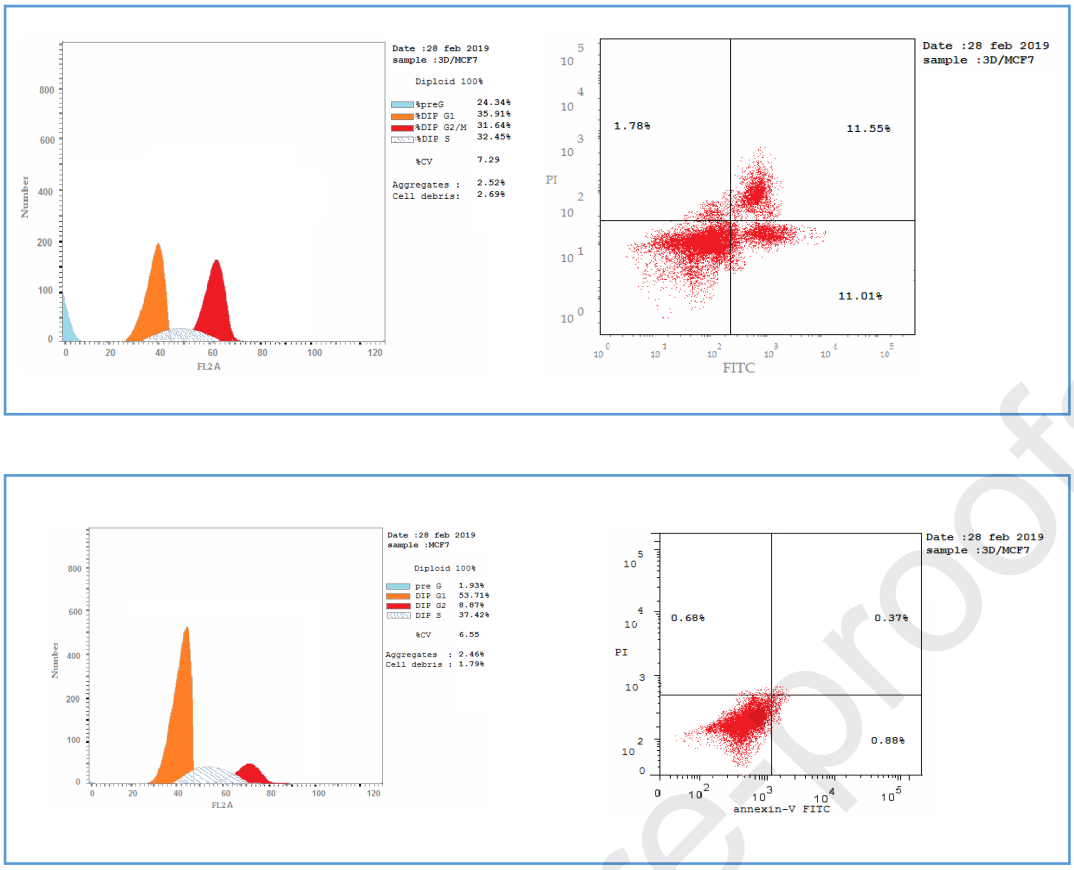

Figure 4. Cell cycle analysis and Apoptosis induction analysis of compound **5a** on MCF-7.

2.2.6. Effect of compounds 5a and 5b on p53 transcription

The transcription effects of **5a** and **5b** on p53 as a possible plausible mechanism for their anticancer efficacy have been evaluated and compared to reference doxorubicin, (Table 6). The results showed an increase of 12-19 in p53 relative to the test cells and that p53 protein levels of 5a and 5b were significantly inductive (991 and 639 pg / mL, respectively) in relation to doxorubicin (1263 pg / mL). A 19-fold increase in the amount of p53 compared with untreated cells in the most active compound **5a**.

Table 6. Effects of compounds **7a**, **7c**, **11** and **doxorubicin** on p53 in MCF-7 cell line.

Compound Number	p53	
	Conc. (pg/ml)	Fold change
5a	991	19.33
5b	639	12.40
Doxorubicin	1263	24.45
Control	51.65	1

2.2.7. Drug likeness profile

Assessment of absorption, distribution, metabolism, and excretion (ADME) became an early routine in drug discovery programs where the availability of computer models constitutes valid alternatives to experiments. The drug likeness profile of the tested compounds **5a-e**, **8a-e** and **9a-e** were predicted using the Swiss ADME website [44]. The results of the drug likeness profile of these compounds are shown in **Tables 7,8**. All the compounds were predicted to have high oral absorption except **9e** due to high molecular weight 546 and molar refractivity 133. All the tested compounds showed no violation to Lipinski (Pfizer) filters except one violation for compounds **8d, 8e** (MlOGP > 4.15), **9d** and **9e** (molecular weight > 500 [45] and no violations to Ghose except one violation for **5e** and **8e**, two violations for **9a,c** and three violations for **9d** and **9e** due to high WLOGP and molecular weight [46], no violation for Veber (GSK) [47], Egan (Pharmacia) [48] and Muegge (Bayer) [49] filters. The compounds were free from alerts for Pan Assay Interfering substances (PAINS) [50]. Total polar surface area (TPSA) values for most compounds are 76.61-98.31, Table 6,7. This consists of "good GIT absorption ". There is a correlation between the molecular weight of compounds and their activity. In addition to low rigidity, this pattern highlighted low molecular weight is favourable. Lipophilicity, together with the molecular weight and the number of hydrogen bond donors and the number of hydrogen acceptors shown by these compounds, plays the role of five.

Table 7: Molecular properties of compounds **5a-e** and **8a-c** predicted using Swiss ADME website.

MOLECULE	5a	5b	5c	5d	5e	8a	8b	8c
MW	405.83	391.81	419.86	426.25	484.73	429.86	415.83	429.86
#HEAVY ATOMS	29	28	30	29	30	31	30	31
#AROMATIC HEAVY ATOMS	16	16	16	16	16	25	25	25
FRACTION CSP3	0.14	0.1	0.17	0.1	0.14	0.13	0.09	0.13
#ROTATABLE BONDS	3	3	4	3	4	1	1	1
#H-BOND ACCEPTORS	5	5	5	5	5	5	5	5
#H-BOND DONORS	0	1	1	1	1	0	1	1
MR	111.58	106.68	116.46	111.69	119.19	117.8	112.9	117.86
TPSA	76.61	87.47	87.47	87.47	87.47	74.31	85.17	85.17
/LOGP	3.68	3.25	3.59	3.42	3.68	3.58	3.16	3.4
XLOGP3	3.42	3.24	3.97	3.86	4.29	3.76	3.58	3.94
WLOGP	4.13	4.12	4.81	4.77	5.27	4.22	4.21	4.52
MLOGP	2.69	2.48	2.9	2.96	3.28	3.99	3.78	3.99
SILICOS-IT LOG P	4.53	5.05	5.97	5.69	6.12	3.59	4.12	4.64
CONSENSUS LOG P	3.69	3.63	4.25	4.14	4.53	3.83	3.77	4.1
ESOL LOG S	-4.72	-4.54	-5.07	-5.12	-5.68	-5.4	-5.22	-5.52
ESOL SOLUBILITY (MG/ML)	7.71E-03	1.14E-02	3.53E-03	3.20E-03	1.02E-03	1.69E-03	2.48E-03	1.30E-03
ESOL SOLUBILITY (MOL/L)	1.90E-05	2.92E-05	8.42E-06	7.50E-06	2.10E-06	3.94E-06	5.97E-06	3.03E-06
ESOL CLASS	Moderately soluble	Moderately soluble	Moderately soluble	Moderately soluble	Moderately soluble	Moderately soluble	Moderately soluble	Moderately soluble
ALI LOG S	-4.71	-4.75	-5.51	-5.39	-5.84	-5.01	-5.05	-5.43
ALI SOLUBILITY (MG/ML)	7.93E-03	6.96E-03	1.30E-03	1.72E-03	7.01E-04	4.17E-03	3.67E-03	1.60E-03
ALI SOLUBILITY (MOL/L)	1.95E-05	1.78E-05	3.11E-06	4.04E-06	1.45E-06	9.69E-06	8.82E-06	3.73E-06
ALI CLASS	Moderately soluble	Moderately soluble	Moderately soluble	Moderately soluble	Moderately soluble	Moderately soluble	Moderately soluble	Moderately soluble
SILICOS-IT LOGSW	-6.84	-7.29	-8.05	-7.87	-8.45	-7.83	-8.28	-8.65
SILICOS-IT SOLUBILITY (MG/ML)	5.91E-05	2.02E-05	3.71E-06	5.72E-06	1.70E-06	6.40E-06	2.19E-06	9.56E-07
SILICOS-IT SOLUBILITY (MOL/L)	1.46E-07	5.16E-08	8.83E-09	1.34E-08	3.52E-09	1.49E-08	5.27E-09	2.22E-09
SILICOS-IT CLASS	Poorly soluble	Poorly soluble	Poorly soluble	Poorly soluble	Poorly soluble	Poorly soluble	Poorly soluble	Poorly soluble
GI ABSORPTION	High	High	High	High	High	High	High	High
BBB PERMEANT	No	No	No	No	No	Yes	No	No
PGP SUBSTRATE	No	No	No	No	No	Yes	Yes	Yes
CYP1A2 INHIBITOR	No	Yes	No	Yes	Yes	No	No	No
CYP2C19 INHIBITOR	Yes	Yes	Yes	Yes	Yes	Yes	Yes	Yes
CYP2C9 INHIBITOR	Yes	Yes	Yes	Yes	Yes	Yes	Yes	Yes
CYP2D6 INHIBITOR	No	No	No	No	No	No	No	No
CYP3A4 INHIBITOR	Yes	Yes	Yes	Yes	Yes	No	No	No
LOG K_P (CM/S)	-6.35	-6.39	-6.04	-6.16	-6.21	-6.25	-6.29	-6.12
LIPINSKI #VIOLATIONS	0	0	0	0	0	0	0	0
GHOSE #VIOLATIONS	0	0	0	0	1	0	0	0
VEBER #VIOLATIONS	0	0	0	0	0	0	0	0
EGAN #VIOLATIONS	0	0	0	0	0	0	0	0

MUEGGE #VIOLATIONS	0	0	0	0	0	0	0	0
BIOAVAILABILITY SCORE	0.55	0.55	0.55	0.55	0.55	0.55	0.55	0.55
PAINS #ALERTS	0	0	0	0	0	0	0	0
BRENK #ALERTS	2	2	2	2	2	0	0	0
LEADLIKENESS #VIOLATIONS	1	1	2	2	2	2	2	2
SYNTHETIC ACCESSIBILITY	4.15	4.08	4.29	4.08	4.19	3.86	3.75	3.86

Table 8: Molecular properties of compounds **8d,e** and **9a-e** predicted using Swiss ADME website.

MOLECULE	8D	8E	9A	9B	9C	9D	9E
MW	450.28	494.73	481.89	467.86	481.89	502.31	546.76
#HEAVY ATOMS	31	31	35	34	35	35	35
#AROMATIC HEAVY ATOMS	25	25	30	30	30	30	30
FRACTION CSP3	0.09	0.09	0.08	0.04	0.08	0.04	0.04
#ROTATABLE BONDS	1	1	2	2	2	2	2
#H-BOND ACCEPTORS	5	5	6	6	6	6	6
#H-BOND DONORS	1	1	0	1	1	1	1
MR	117.91	120.6	130.54	125.63	130.6	130.64	133.33
TPSA	85.17	85.17	87.45	98.31	98.31	98.31	98.31
ILOGP	3.38	3.49	3.88	3.56	3.78	3.76	3.89
XLOGP3	4.21	4.27	4.13	3.94	4.31	4.57	4.63
WLOGP	4.87	4.98	5.18	5.17	5.47	5.82	5.93
MLOGP	4.26	4.36	3.65	3.45	3.65	3.91	4.01
SILICOS-IT LOG P	4.76	4.79	3.97	4.5	5.02	5.13	5.17
CONSENSUS LOG P	4.29	4.38	4.16	4.12	4.45	4.64	4.73
ESOL LOG S	-5.81	-6.13	-5.93	-5.74	-6.05	-6.34	-6.65
ESOL SOLUBILITY (MG/ML)	6.90E-04	3.68E-04	5.64E-04	8.44E-04	4.34E-04	2.32E-04	1.23E-04
ESOL SOLUBILITY (MOL/L)	1.53E-06	7.44E-07	1.17E-06	1.80E-06	9.01E-07	4.62E-07	2.24E-07
ESOL CLASS	Moderately soluble	Poorly soluble	Moderately soluble	Moderately soluble	Poorly soluble	Poorly soluble	Poorly soluble
ALI LOG S	-5.71	-5.77	-5.67	-5.7	-6.09	-6.36	-6.42
ALI SOLUBILITY (MG/ML)	8.81E-04	8.39E-04	1.02E-03	9.24E-04	3.93E-04	2.20E-04	2.08E-04
ALI SOLUBILITY (MOL/L)	1.96E-06	1.70E-06	2.12E-06	1.98E-06	8.16E-07	4.39E-07	3.80E-07
ALI CLASS	Moderately soluble	Moderately soluble	Moderately soluble	Moderately soluble	Poorly soluble	Poorly soluble	Poorly soluble
SILICOS-IT LOGSW	-8.86	-9.05	-9.12	-9.57	-9.94	-10.15	-10.33
SILICOS-IT SOLUBILITY (MG/ML)	6.20E-07	4.41E-07	3.67E-07	1.26E-07	5.49E-08	3.56E-08	2.55E-08
SILICOS-IT SOLUBILITY (MOL/L)	1.38E-09	8.91E-10	7.62E-10	2.69E-10	1.14E-10	7.10E-11	4.66E-11
SILICOS-IT CLASS	Poorly soluble	Poorly soluble	Poorly soluble	Poorly soluble	Poorly soluble	Insoluble	Insoluble
GI ABSORPTION	High	High	High	High	High	High	Low
BBB PERMEANT	No	No	No	No	No	No	No
PGP SUBSTRATE	Yes	Yes	Yes	Yes	Yes	Yes	Yes
CYP1A2 INHIBITOR	No	No	No	No	No	No	No
CYP2C19 INHIBITOR	Yes	Yes	No	No	No	No	No

CYP2C9 INHIBITOR	Yes	Yes	Yes	No	No	No	No
CYP2D6 INHIBITOR	No	No	No	No	No	No	No
CYP3A4 INHIBITOR	No	No	No	No	No	No	No
LOG K_P (CM/S)	-6.06	-6.29	-6.31	-6.36	-6.18	-6.12	-6.35
LIPINSKI #VIOLATIONS	1	1	0	0	0	1	1
GHOSE #VIOLATIONS	0	1	2	0	2	3	3
VEBER #VIOLATIONS	0	0	0	0	0	0	0
EGAN #VIOLATIONS	0	0	0	0	0	0	0
MUEGGE #VIOLATIONS	0	0	0	0	0	0	0
BIOAVAILABILITY SCORE	0.55	0.55	0.55	0.55	0.55	0.55	0.55
PAINS #ALERTS	0	0	0	0	0	0	0
BRENK #ALERTS	0	0	0	0	0	0	0
LEAD LIKENESS #VIOLATIONS	2	2	2	2	2	2	2
SYNTHETIC ACCESSIBILITY	3.76	3.77	4.11	4	4.11	4	4.01

3. Conclusion

Pyrano[3,2-*c*]quinoline derivatives have been synthesized and converted to heteroannulated triazolo-pyrimidines, containing quinoline, pyran, 1,2,4-triazine and pyrimidine structures. Most of the new compounds showed moderate to weak antiproliferative activity on most cancer cell lines, especially leukemia and breast cancer cell lines. The open chain formimidic acid ethyl ester is slightly more potent than heteroannulated systems. The most active compounds were further investigated for caspase activation, Bax activation and Bcl-2 down regulation compared to doxorubicin as a standard and exhibited cell cycle arrest at the Pre-G1 and G2/M phases. p53 assay results showed a 19-fold increase in the amount of p53 compared with untreated cells in the most active compound **5a**.

Conflict of interest: The authors declare no conflict of interest.

4. Experimental

4.1. Chemistry

General details: See Appendix A

Starting materials

4-Hydroxy-2-quinolones **1a-e** [51, 52] and 2-(4-chlorobenzylidene) malononitrile **2** [53] were synthesized according to reported literature.

4.1.1. General method for synthesis of compounds 3a-e

To a solution of quinolone derivatives **1a-e** (1 mmol) in dry ethanol (30 mL), 2-(4-chlorobenzylidene) malononitrile **2** (0.188 g, 1 mmol) was added. The reaction mixture was heated under reflux for 1–2 h (monitored by TLC). After reaction completion, the precipitated solid was filtered, dried, and crystallized from methanol to afford compounds **3a-e**.

4.1.1.1 2-Amino-4-(4-chlorophenyl)-6-methyl-5-oxo-5,6-dihydro-4H-pyrano[3,2-c]quinoline-3-carbonitrile (3a) [52].

Yield 0.312 g (86%); mp 280–282 °C, IR (KBr) υ_{max}/cm^{-1} 3388, 3300, 2964, 1636.

4.1.1.2. 2-Amino-4-(4-chlorophenyl)-5-oxo-5,6-dihydro-4H-pyrano[3,2-c]quinoline-3-carbonitrile (3b) [51].

Yield 0.310 g (89%); mp 310–312 °C, IR (KBr) υ_{max}/cm^{-1} 3399, 3322, 3164, 1686.

4.1.1.3. 2-Amino-4-(4-chlorophenyl)-9-methyl-5-oxo-5,6-dihydro-4H-pyrano[3,2-c]quinoline-3-carbonitrile (3c)

Yield 0.345 g (90%); mp 284–285 °C, IR (KBr) υ_{max}/cm^{-1} 3387, 2930, 2234, 1637. ^{1}HNMR δ_H 11.72 (s; 1H; NH), 7.72 (bs, 1H; H-10), 7.42 (dd, *J*= 8.4, 1.7, 1H; H-8); 7.35 (d, *J* = 8.4, 2H; H-*m*); 7.30 (bs, 2H; H-2a), 7.24 (d, *J* = 8.1, 1H; H-7), 7.23 (d, *J* = 8.5, 2H; H-*o*), 4.51 (s,1H;

H-4), 2.39 (s, 3H; H-9a). ^{13}C NMR δ_C 160.22 (C-5), 158.94 (C-2), 151.07 (C-10b), 143.40 (C-*i*), 135.88 (C-6a), 132.46 (C-8), 131.21 (C-*p*), 131.08 (C-9), 129.28 (2C-*o*), 128.27 (2C-*m*), 121.22 (C-10), 119.61 (C-3a), 115.29 (C-7), 111.82 (C-10a), 108.97 (C-4a), 57.30 (C-3), 36.24 (C-4), 20.62 (C-6b). MS m/z (%): 363/365 (M^+/M+2, 22/7), 286 (73), 252 (49), 77 (100). Anal. Calcd for $C_{20}H_{14}ClN_3O_2$ (363.80): C, 66.03; H, 3.88; N, 11.55. Found: C, 66.33; H, 3.99; N, 11.82.

4.1.1.4. 2-Amino-9-chloro-4-(4-chlorophenyl)-5-oxo-5,6-dihydro-4H-pyrano[3,2-c]quinoline-3-carbonitrile (3d)

Yield 0.337 g (88%); mp 275–277 °C, IR (KBr) υ_{max}/cm^{-1} 3397, 3312, 2186, 1648. ^{1}HNMR δ_H 11.93 (s; 1H; H-6), 7.950 (s, 1H; H-10), 7.64 (d, *J* = 8.8, 1H; H-8); 7.35 (d, *J* = 8.5, 2H; H-*m*); 7.35 (d, *J* = 8.7, 1H; H-7), 7.37 (b, 2H; H-2a), 7.24 (d, *J* = 8.5, 2H; H-*o*), 4.52 (s,1H; H-4). ^{13}CNMR δ_C 160.18 (C-5), 158.72 (C-2), 150.28 (C-10b), 143.05 (C-*i*), 136.56 (C-6a), 131.32 (C-8), 131.19 (C-*p*), 129.37 (2C-*o*), 128.30(2C-*m*), 126.16 (C-9), 121.13 (C-10), 119.44 (C-3a), 117.36 (C-7), 113.20 (C-10a), 110.04 (C-4a), 57.23 (C-3), 36.24 (C-4). MS m/z (%): 384/386 (M^+/M+2, 6/2), 272 (17), 75 (85), 66 (100). Anal. Calcd for $C_{19}H_{11}Cl_2N_3O_2$ (384.22): C, 59.40; H, 2.89; N, 10.94. Found: C, 59.61; H, 2.63; N, 10.75.

4.1.1.5. 2-Amino-9-bromo-4-(4-chlorophenyl)-5-oxo-5,6-dihydro-4H-pyrano[3,2-c]quinoline-3-carbonitrile (3e)

Yield 0.363 g (85%); mp 279–281 °C, IR (KBr) υ_{max}/cm^{-1} 3380, 3301, 2150, 1660. ^{1}HNMR δ_H 11.92 (s; 1H; H-6), 8.20 (s, 1H; H-10), 7.75 (d, *J* = 7.5, 1H; H-8); 7.34 (m, 3H; H-*m,* 7); 7.25 (m, 4H; H-*o*, 2a), 4.51 (s, 1H; H-4). ^{13}CNMR δ_C 160.16 (C-5), 158.72 (C-2), 150.19 (C-10b), 143.06 (C-*i*), 136.87 (C-6a), 133.85 (C-8), 131.32 (C-*p*), 129.38 (2C-*o*), 128.31(2C-*m*), 124.12 (C-10), 119.44 (C-3a), 117.57 (C-7), 113.84 (C-9), 113.67 (C-10a), 110.00 (C-4a), 57.24 (C-3), 36.23 (C-4). MS m/z (%): 428/430 (M^+/M+2, 12/4), 361 (50), 316 (56), 74 (86), 66 (100).

Anal. Calcd for $C_{19}H_{11}BrClN_3O_2$ (428.67): C, 53.24; H, 2.59; N, 9.80. Found: C, 53.43; H, 2.91; N, 9.62.

4.1.2. General method for synthesis of (5a-e)

A solution of compounds **3a-e** (0.001 mol) and trimethyl orthoformate **4a** or triethyl orthoformate **4b** (1 ml) containing 3 drops of acetic anhydride was refluxed for 6-8 h. The reaction mixture was cooled and then poured onto ice water. The obtained solid was recrystallized from methanol to afford the target compounds **5a-e**.

4.1.2.1. Methyl (E)-N-(4-(4-chlorophenyl)-3-cyano-6-methyl-5-oxo-5,6-dihydro-4H-pyrano-[3,2-c]quinolin-2-yl) formimidate(5a)

Yield: 0.304 g (75%); mp 235–237 °C, IR (KBr) υ_{max}/cm^{-1} 2976, 2220, 1640. ^{1}HNMR δ_H 8.97 (s, 1H; H-2b), 8.24 (dd, *J* = 8.0, 1.2, 1H; H-10), 7.74 (ddd, *J*= 8.6, 7.2, 1.4, 1H; H-8), 7.59 (d, *J* = 8.4, 1H; H-7), 7.39 (m, 1H; H-9), 7.38 (d, *J* = 8.5, 2H; H-*m*), 7.34 (d, *J* = 8.7, 2H; H-*o*), 4.79 (s, 1H; H-4), 3.93 (s, 3H; H-2d), 3.55 (s, 3H; H-6b). ^{13}CNMR δ_C 162.72 (C-2b), 159.64 (C-5), 155.92 (C-2), 150.47 (C-10b), 141.48 (C-*i*), 138.79 (C-6a), 131.91 (C-8), 131.10 (C-*p*), 130.03 (2C-*o*), 128.43 (2C-*m*), 123.09 (C-10), 122.35 (C-9), 117.06 (C-3a), 114.89 (C-7), 112.58 (C-10a), 107.25 (C-4a), 82.18 (C-3), 54.94 (C-2d), 38.27 (C-4), 29.34 (C-6b). MS m/z (%): 405/407 (M^+ /M+2, 50/20), 291 (48), 164 (56), 49 (100). Anal. Calcd for $C_{22}H_{16}ClN_3O_3$ (405.84): C, 65.11; H, 3.97; N, 10.35; Found: C, 65.44; H, 3.70; N, 10.52.

4.1.2.2. Methyl (E)-N-(4-(4-chlorophenyl)-3-cyano-5-oxo-5,6-dihydro-4H-pyrano[3,2-c]-quinolin-2-yl)formimidate (5b)

Yield: 0.281 g (70%); mp 241–243 °C, IR (KBr) υ_{max}/cm^{-1} 3178, 2210, 1617. ^{1}HNMR δ_H 11.86 (s, 1H; H-6), 8.95 (s, 1H; H-2b), 8.12 (d, *J* = 7.9, 1H; H-10), 7.59 (d"t", J_d = 1.2, $J_{"t"}$ = 7.7, 1H; H-8), 7.39 (d, *J* = 8.6, 2H; H-*m*), 7.332 (d, *J* = 6.8, 1H; H-7), 7.330 (d, *J* = 8.5, 2H; H-*o*), 7.27

("t", *J* = 7.6, 1H; H-9), 4.75 (s, 1H; H-4), 3.92 (s, 3H; H-2d). ^{13}CNMR δ_C 162.23 (C-2), 159.81 (C-2b), 155.48 (C-5), 151.02 (C-10b), 137.48 (C-8), 131.42 (C-*i*), 131.03 (C-*p*), 131.01 (C-6a), 129.50 (2C-*o*), 127.99 (2C-*m*), 122.20 (C-9), 121.64 (C-3a), 116.66 (C-4a), 114.78 (C-7), 111.42 (C-10), 107.30 (C-10a), 81.94 (C-3), 54.45 (C-2d), 37.21 (C-4). MS m/z (%): 391/393 (M^+/M+2, 12/4), 348 (18), 238 (66), 92 (100). Anal. Calcd for $C_{21}H_{14}ClN_3O_3$ (391.81): C, 64.38; H, 3.60; N, 10.72. Found: C, 64.77; H, 3.89; N, 11.05.

4.1.2.3. Ethyl (E)-N-(4-(4-chlorophenyl)-3-cyano-9-methyl-5-oxo-5,6-dihydro-4H-pyrano-[3,2-c]quinolin-2-yl) formimidate (5c)

Yield: 0.318 g (76%); mp 252–253 °C, IR (KBr) υ_{max}/cm^{-1} 3154, 2940, 2243. ^{1}HNMR δ_H 11.77 (s, 1H; H-6), 8.94 (s, 1H; H-2b), 7.89 (bs, 1H; H-10), 7.41 (dd, *J*= 8.7, 1.4; 1H; H-8), 7.38 (d, *J* = 8.5; 2H; H-*m*), 7.31 (d, *J* = 8.5, 2H; H-*o*), 7.23 (d, *J* = 8.4, 1H; H-7), 7.330 (4.72 (s, 1H; H-4), 4.37 (q, *J* = 7.0, 2H; H-2d), 2.40 (s, 3H; H-9a), 1.34 (t, *J* = 7.1, 3H; H-2e). ^{13}CNMR δ_C 161.80 (C-2), 159.65 (C-2b), 155.70 (C-5), 150.87 (C-10b), 141.16 (C-6a), 135.51 (C-8), 132.25 (C-9), 131.36 (C-*i*), 131.02 (C-*p*), 129.46 (2C-*o*), 127.98 (2C-*m*), 121.34 (C-3a), 116.74 (C-4a), 114.72 (C-7), 111.29 (C-10), 107.19 (C-10a), 81.35 (C-3), 63.48 (C-2d), 37.21 (C-4), 19.91 (C-9a), 13.34 (C-2e). MS m/z (%): 419/421 (M^+ /M+2, 18/6), 308 (22), 252 (60), 77 (100). Anal. Calcd for $C_{23}H_{18}ClN_3O_3$ (419.87): C, 65.80; H, 4.32; N, 10.01. Found: C, 65.42; H, 4.68; N, 10.28.

4.1.2.4. Methyl (E)-N-(9-chloro-4-(4-chlorophenyl)-3-cyano-5-oxo-5,6-dihydro-4H-pyrano[3,2-c]quinolin-2-yl)formimidate (5d)

Yield: 0.310 g (73%); mp 258–260 °C, IR (KBr) υ_{max}/cm^{-1} 3190, 2251, 1649. ^{1}HNMR δ_H11.98 (s, 1H; H-6), 9.05 (s, 1H; H-2b), 8.20 (bs, 1H; H-10), 7.63 (dd, *J*= 8.8, 2.2, 1H; H-8), 7.38 (d, *J* = 8.3, 2H; H-*m*), 7.329 (d, *J* = 8.5, 2H; H-*o*), 7.326 (d, *J* = 8.7, 1H; H-7), 4.75 (s, 1H; H-4), 3.91 (s, 3H; H-2d). ^{13}CNMR δ_C 162.69 (C-2), 159.58 (C-2b), 155.39 (C-5), 151.20 (C-10b),

140.85 (C-6a), 136.16 (C-8), 131.49 (C-*i*), 131.08 (C-*p*), 129.54 (2C-*o*), 128.01 (2C-*m*), 126.06 (C-9), 121.36 (C-3a), 116.77 (C-4a), 116.58 (C-7), 112.66 (C-10), 108.39 (C-10a), 81.72 (C-3), 54.36 (C-2d), 37.20 (C-4). MS m/z (%): 426/428 (M^+ /M+2, 78/26), 382 (32), 314 (100), 75 (87). Anal. Calcd for $C_{21}H_{13}Cl_2N_3O_3$ (426.25): C, 59.17; H, 3.07; N, 9.86. Found: C, 59.54; H, 3.20; N, 9.68.

4.1.2.5. Ethyl (E)-N-(9-bromo-4-(4-chlorophenyl)-3-cyano-5-oxo-5,6-dihydro-4H-pyrano-[3,2-c] quinolin-2-yl)formimidate (5e)

Yield: 0.339 g (70%); mp 266–268 °C, IR (KBr) υ_{max}/cm^{-1} 3223, 2890, 2235, 1669. ^{1}HNMR δ_H 11.98 (s, 1H; NH-6), 9.00 (s, 1H; H-2b), 8.29 (d, *J* = 1.9, 1H; H-10), 7.75 (dd, *J* = 8.8, 2.2, 1H; H-8), 7.39 (d, *J* = 8.5, 2H; H-*m*), 7.33 (d, *J* = 8.5, 2H; H-*o*), 7.28 (d, *J* = 8.8, 1H; H-7), 4.75 (s, 1H; H-4), 4.37 (q, *J* = 7.1, 2H; H-2d), 1.35 (t, *J* = 7.1, 3H; H-2e). ^{13}CNMR δ_C 162.71 (C-2b), 160.02 (C-5), 156.12 (C-2), 150.59 (C-10b), 141.35 (C-*i*), 136.99 (C-6a), 134.21 (C-8), 131.94 (C-*p*), 129.97 (2C-*o*), 128.46 (2C-*m*), 124.59 (C-10), 117.45 (C-3a), 117.06 (C-7), 114.20 (C-9), 113.58 (C-10a), 108.83 (C-4a), 81.77 (C-3), 63.92 (C-2d), 37.65 (C-4), 13.81 (C-2e). MS m/z (%):484/486 (M^+ /M+2, 10/10), 428 (14), 318 (100), 316 (74). Anal. Calcd for $C_{22}H_{15}BrClN_3O_3$ (484.73): C, 54.51; H, 3.12; N, 8.67. Found: C, 54.32; H, 3.36; N, 8.74.

4.1.3. General method for the synthesis of compounds (8a-e)

A mixture of formimidate derivatives **5a-e** (0.001 mol) and acetohydrazide **6** (0.001 mol) in acetic acid (30 mL) was refluxed overnight. The mixture was cooled, and the solvent was removed under reduced pressure to afford the target compounds **8a-e** and purified by crystallization from acetic acid.

4.1.3.1. 14-(4-Chlorophenyl)-2,12-dimethyl-12,14-dihydro-13H-[1,2,4]triazolo[1'',5'':1',6']-pyrimido[5',4':5,6]pyrano[3,2-c]quinolin-13-one (8a)

Yield: 0.310 g (73%); mp 235–237 °C, IR (KBr) υ_{max}/cm^{-1} 3167, 1677. ^{1}HNMR δ_H 10.01 (bs, 1H; H-5), 8.90 (d, *J* = 8.1, 1H; H-8), 8.36 ("t", *J* = 7.8, 1H; H-10), 8.18 (d, *J* = 8.6, 1H; H-11), 8.12 ("t", *J* = 7.6, 1H; H-9), 7.87 (d, *J* = 8.0; 2H, H-*m*), 7.69 (d, *J* = 8.0, 2H; H-*o*), 6.38 (s, 1H; H-14), 4.33 (s, 3H; H-12a), 3.20 (s, 3H; H-2a). ^{13}CNMR δ_C 165.06 (C-13), 161.27 (C-2), 160.66 (C-6a), 155.88 (C-7a), 149.56 (C-14b), 143.83 (C-5), 141.02 (C-11a), 139.28 (C-*p*), 138.37 (C-*i*), 136.25 (C-10), 132.02 (2C-*m*), 131.82 (2C-*o*), 127.75 (C-9), 125.39 (C-8), 117.72 (C-7), 116.06 (C-7b), 109.91 (C-13a), 104.94 (C-14a), 38.36 (C-14), 32.70 (C-12a), 12.50 (C-2a). MS m/z (%):429/431 (M^+ /M+2, 56/18), 318 (100), 111 (16), 75 (58). Anal. Calcd for $C_{23}H_{16}ClN_5O_2$ (429.86): C, 64.27; H, 3.75; N, 16.29. Found: C, 63.94; H, 3.90; N, 16.60.

4.1.3.2. 14-(4-Chlorophenyl)-2-methyl-12,14-dihydro-13H-[1,2,4]triazolo[1'',5'':1',6']-pyrimido[5',4':5,6]pyrano[3,2-c]quinolin-13-one (8b)

Yield: 0.337 g (78%); mp 245–247 °C, IR (KBr) υ_{max}/cm^{-1} 3315, 3100, 1663. ^{1}HNMR δ_H 12.05 (s, 1H; NH), 10.06 (s, 1H; H-5), 8.90 (d, *J* = 7.9, 1H; H-8), 8.35 (d"t", J_d= 1.0, $J_{"t"}$ = 7.8, 1H; H-10), 8.18 ("t", *J* = 7.6, 1H; H-9), 8.12 (d, J = 8.4; 1H, H-11), 7.84 (d, *J* = 8.6, 2H; H-*o*), 7.72 (d, *J* = 8.5, 2H; H-*m*), 6.42 (s, 1H; H-14), 3.21 (s, 3H, H-2a). ^{13}CNMR δ_C 164.74 (C-13), 161.67 (C-2), 160.50 (C-6a), 158.04 (C-7a), 149.68 (C-14b), 143.95 (C-5), 138.61 (C-*i*), 138.50 (C-*p*), 136.69 (C-10), 136.10 (C-11a), 132.04 (2C-*o*), 131.82 (2C-*m*), 129.01 (C-9), 124.83 (C-8), 119.37 (C-11), 115.99 (C-7b), 108.78 (C-13a), 104.58 (C-14a), 37.41 (C-14), 12.54 (C-2a). MS m/z (%): 415/417 (M^+ /M+2, 42/14), 304 (92), 111 (34), 75 (100). Anal. Calcd for $C_{22}H_{14}ClN_5O_2$ (415.84): C, 63.54; H, 3.39; N, 16.84. Found: C, 63.67; H, 3.60; N, 16.67.

4.1.3.3. 14-(4-Chlorophenyl)-2,9-dimethyl-12,14-dihydro-13H-[1,2,4]triazolo[1'',5'':1',6']-pyrimido[5',4':5,6]pyrano[3,2-c]quinolin-13-one (8c)

Yield: 0.337 g (78%); mp 250–253 °C, IR (KBr) υ_{max}/cm^{-1} 3324, 3175, 1656. ^{1}HNMR δ_H 10.08 (bs, 1H; H-5), 8.73 (d, *J* = 1.6, 1H; H-8), 8.24 (d, *J* = 8.2, 1H; H-10), 8.07 (d, *J* = 8.5, 1H; H-

11), 7.85 (d, *J* = 7.9, 2H; H-*m*), 7.74 (d, *J* = 7.8, 2H; H-*o*), 6.44 (s, 1H; H-14), 3.22 (s, 3H, H-2a), 3.09 (s, 3H, H-9a). ^{13}CNMR δ_C 164 (C-13), 161.75 (C-2), 160.49 (C-6a), 158.17 (C-7a), 149.73 (C-14b), 144.02 (C-5), 141.11 (C-9), 138.72 (C-10), 138.58 (C-*i*), 137.58 (C-*p*), 136.72 (C-11a), 132.04 (2C-*m*), 131.88 (2C-*o*), 123.96 (C-8), 119.47 (C-11), 116.26 (C-7b), 107.17 (C-13a), 104.61 (C-14a), 37.39 (C-14), 21.90 (C-9a), 12.59 (C-2a). MS m/z (%): 429/431 (M^+ /M+2, 54/18), 318 (100), 289 (12), 195 (10). Anal. Calcd for $C_{23}H_{16}ClN_5O_2$ (429.86): C, 64.27; H, 3.75; N, 16.29. Found: C, 64.43; H, 3.50; N, 16.58.

4.1.3.4. 9-Chloro-14-(4-chlorophenyl)-2-methyl-12,14-dihydro-13H-[1,2,4]triazolo-[1'',5'':1',6']pyrimido[5',4':5,6]pyrano[3,2-c]quinolin-13-one (8d)

Yield: 0.319 g (71%); mp 243–245 °C, IR (KBr) υ_{max}/cm^{-1} 3319, 3150, 1643. ^{1}HNMR δ_H 12.05 (s, 1H; NH), 10.05 (bs, 1H; H-5), 8.83 (d, *J* = 1.6, 1H; H-8), 8.26 (dd, *J* = 8.8, 1.7, 1H; H-10), 8.02 (d, *J* = 8.9; 1H, H-11), 7.84 (d, *J* = 8.4, 2H; H-*m*), 7.73 (d, *J* = 8.3, 2H; H-*o*), 6.40 (s, 1H; H-14), 3.21 (s, 3H; H-2a). ^{13}CNMR δ_C 166.33 (C-13), 161.72 (C-6a), 160.35 (C-2), 156.42 (C-7a), 149.68 (C-14b), 143.83 (C-5), 138.47 (C-*p*), 137.08 (C-*i*), 136.73 (C-10), 136.73 (C-11a), 135.17 (C-9), 132.03 (2C-*m*), 131.76 (2C-*o*), 124.12 (C-8), 120.52 (C-11), 116.59 (C-7b), 110.32 (C-13a), 104.54 (C-14a), 37.47 (C-14), 12.50 (C-2a). MS m/z (%): 450/452 (M^+ /M+2, 28/10), 338 (100), 199 (8), 75 (14). Anal. Calcd for $C_{22}H_{13}Cl_2N_5O_2$ (450.28):C, 58.68; H, 2.91; N, 15.55. Found: C, 59.08; H, 2.58; N, 15.76.

4.1.3.5.9-bromo-14-(4-chlorophenyl)-2-methyl-12H-[1,2,4]triazolo[1'',5'':1',6'] pyrimido[5',4':5,6]pyrano[3,2-c]quinolin-13(14H)-one (8e)

Yield: 0.325 g (74%); mp 233–235 °C, IR (KBr) υ_{max}/cm^{-1} 3310, 3140, 1633. ^{1}HNMR δ_H 12.07 (s, 1H; NH), 10.11 (bs, 1H; H-5), 8.85 (d, *J* = 1.7, 1H; H-8), 8.35 (d, *J* = 8.8, 1H; H-10), 7.90 (d, *J* = 8.48; 1H, H-11), 7.84 (d, *J* = 8.4, 2H; H-*o*), 7.63 (d, *J* = 8.3, 2H; H-*m*), 6.44 (s, 1H; H-14), 3.27 (s, 3H; H-2a). ^{13}CNMR δ_C 164.45 (C-13), 161.84 (C-2), 160.80 (C-6a), 158.66 (C-

7a), 149.92 (C-14b), 144.29 (C-5), 139.83 (C-10), 138.94 (C-*p*), 138.73 (C-*i*), 137.83 (C-11a), 132.44 (2C-*m*), 131.13 (2C-*o*), 127.73 (C-8), 122.12 (C-9), 120.93 (C-11), 117.77 (C-7b), 110.62 (C-13a), 104.79 (C-14a), 37.82 (C-14), 12.87 (C-2a). MS m/z (%): 494/496 (M^+/M+2, 16/15), 479 (70), 258 (100), 75 (98). Anal. Calcd for $C_{22}H_{13}BrClN_5O_2$ (494.73): C, 53.41; H, 2.65; N, 14.16. Found: C, 53.64; H, 2.80; N, 14.01.

4.1.4. General method for the synthesis of compounds (9a-e)

A mixture of formimidate derivatives **5a-e** (0.001 mol) and furan-2-carbohydrazide **7** (0.001 mol) in acetic acid (30 mL) was refluxed for 12 hr. The mixture was cooled, and the solvent was removed under reduced pressure to afford the target compounds **9a-e** and purified by crystallization from acetic acid.

4.1.4.1. 14-(4-Chlorophenyl)-2-(furan-2-yl)-12-methyl-12,14-dihydro-13H-[1,2,4]triazolo-[1'',5'':1',6']pyrimido[5',4':5,6]pyrano[3,2-c]quinolin-13-one (9a)

Yield: 0.379 g (79%); mp 247–249 °C, IR (KBr) υ_{max}/cm^{-1} 3165, 1654. ^{1}HNMR δ_H 10.10 (s, 1H; H-5), 8.92 (d, *J* = 8.1, 1H; H-8), 8.37 ("t", *J* = 7.9, 1H; H-10), 8.24 (bs, 1H; H-2d), 8.19 (d, *J* = 8.7, 1H; H-11), 8.13 ("t", *J* = 7.7, 1H; H-9), 8.07 (d, *J* = 3.6, 1H; H-2b), 7.93 (d, *J* = 8.3, 2H; H-*m*), 7.71 (d, *J* = 8.2, 2H; H-*o*), 7.21 (dd, *J* = 3.4, 1.5, 1H; H-2c), 6.51 (s, 1H; H-14), 4.36 (s, 3H; H-12a).^{13}CNMR δ_C 165.04 (C-13), 160.65 (C-6a), 156.14 (C-7a), 153.73 (C-2), 151.30 (C-2d), 150.41 (C-14b), 143.78 (C-5), 141.19 (C-11a), 140.04 (C-2a), 139.67 (C-*p*), 138.28 (C-*i*), 136.19 (C-10), 132.07 (2C-*m*), 131.87 (2C-*o*), 127.70 (C-9), 125.47 (C-8), 121.58 (C-2b), 117.66 (C-11), 116.27 (C-7b), 115.85 (C-2c), 110.42 (C-13a), 105.66 (C-14a), 38.26 (C-14), 32.84 (C-12a). MS m/z (%):481/483 (M^+ /M+2, 21/7), 389 (6), 370 (100), 289 (38).Anal. Calcd for $C_{26}H_{16}ClN_5O_3$ (481.90): C, 64.80; H, 3.35; N, 14.53. Found: C, 65.07; H, 3.52; N, 14.86.

4.1.4.2. 14-(4-chlorophenyl)-2-(furan-2-yl)-12H-[1,2,4]triazolo[1'',5'':1',6']pyrimido-[5',4':5,6]pyrano[3,2-c]quinolin-13(14H)-one (9b)

Yield: 0.356 g (71%); mp 231–233 °C, IR (KBr) υ_{max}/cm^{-1} 3090, 1680. ^{1}HNMR δ_H 10.12 (s, 1H; H-5), 8.89 (d, *J* = 8.2, 1H; H-8), 8.33 (t, *J* = 7.8, 1H; H-10), 8.20 (bs, 1H; H-2d), 8.16 (t, *J* = 7.8, 1H; H-9), 8.11 (d, *J* = 8.3, 1H; H-11), 8.03 (d, *J* = 3.6, 1H; H-2b), 7.86 (d, *J* = 8.4, 2H; H-*m*), 7.70 (d, *J* = 8.2, 2H; H-*o*), 7.17 (dd, *J* = 3.5, 1.6, 1H; H-2c), 6.50 (s, 1H; H-14). ^{13}CNMR δ_C 164.00 (C-13), 161.58 (C-2), 158.66 (C-6a), 156.91 (C-7a), 149.65 (C-2d), 149.65 (C-14b), 142.47 (C-5), 138.66 (C-2a), 137.37 (C-*i*), 137.09 (C-*p*), 136.81 (C-11a), 135.23 (C-10), 130.52 (2C-*m*), 130.26 (2C-*o*), 127.81 (C-9), 123.36 (C-8), 119.92 (C-2b), 118.00 (C-11), 114.72 (C-7b), 114.24 (C-2c), 107.53 (C-13a), 103.68 (C-14a), 35.69 (C-14). MS m/z (%): 467/469 (M^+/M+2, 89/30), 420 (81), 43 (100), 44 (84). Anal. Calcd for $C_{25}H_{14}ClN_5O_3$ (476.86): C, 64.18; H, 3.02; N, 14.97. Found: C, 64.38; H, 3.16; N, 14.80.

4.1.4.3. 14-(4-chlorophenyl)-2-(furan-2-yl)-9-methyl-12,14-dihydro-13H-[1,2,4]triazolo-[1'',5'':1',6']pyrimido[5',4':5,6]pyrano[3,2-c]quinolin-13-one (9c)

Yield: 0.336 g (70%); mp 237–239 °C, IR (KBr) υ_{max}/cm^{-1} 3100, 1690. ^{1}HNMR δ_H 10.14 (s, 1H; H-5), 8.73 (bs, 1H; H-8), 8.23 (d, *J* = 8.6, 1H; H-10), 8.22 (bs, 1H; H-2d), 8.08 (d, *J* = 8.6, 1H; H-11), 8.05 (d, *J* = 3.6, 1H; H-2b), 7.88 (d, *J* = 8.2, 2H; H-*m*), 7.72 (d, *J* = 8.2, 2H; H-*o*), 7.19 (dd, *J* = 3.5, 1.5, 1H; H-2c), 6.52 (s, 1H; H-14), 3.08 (s, 3H; H-9a). ^{13}CNMR δ_C 164.03 (C-13), 161.69 (C-2), 158.56 (C-6a), 157.03 (C-7a), 149.66 (C-2d), 149.25 (C-14b), 142.53 (C-5), 139.81 (C-9), 138.75 (C-2a), 137.33 (C-*i*), 137.30 (C-*p*), 136.88 (C-10), 135.18 (C-11a), 130.53 (2C-*m*), 130.31 (2C-*o*), 122.50 (C-8), 119.93 (C-2b), 118.11 (C-11), 115.01 (C-7b), 114.27 (C-2c), 106.97 (C-13a), 103.69 (C-14a), 35.65 (C-14), 20.46 (C-9). MS m/z (%):481/483 (M^+/M+2, 18/6), 419 (100), 164 (99), 157 (50). Anal. Calcd for $C_{26}H_{16}ClN_5O_3$ (481.90): C, 64.80; H, 3.35; N, 14.53. Found: C, 65.02; H, 3.66; N, 14.90.

4.1.4.4. 9-Chloro-14-(4-chlorophenyl)-2-(furan-2-yl)-12,14-dihydro-13H-[1,2,4]triazolo-[1'',5'':1',6']pyrimido[5',4':5,6]pyrano[3,2-c]quinolin-13-one (9d)

Yield: 0.381 g (76%); mp 256–258 °C, IR (KBr) υ_{max}/cm^{-1} 3323, 1654. ^{1}HNMR δ_H 12.07 (bs, 1H; NH), 10.14 (s, 1H; H-5), 8.84 (d, *J* = 2.0, 1H; H-8), 8.27 (dd, *J* = 8.9, 2.1, 1H; H-10), 8.23 (d, *J* = 1.0, 1H; H-2d), 8.06 (d, *J* = 4.2, 1H; H-2b), 8.05 (d, *J* = 9.3, 1H; H-11), 7.89 (d, *J* = 8.4, 2H; H-*m*), 7.74 (d, *J* = 8.5, 2H; H-*o*), 7.21 (dd, *J* = 3.5, 1.5, 1H; H-2c), 6.51 (s, 1H; H-14). ^{13}CNMR δ_C 164.23 (C-13), 159.93 (C-6a), 156.68 (C-7a), 154.19 (C-2), 150.99 (C-2d), 150.56 (C-14b), 143.76 (C-5), 140.08 (C-2a), 138.67 (C-*p*), 138.17 (C-*i*), 136.95 (C-11a), 136.68 (C-10), 135.23 (C-9), 131.93 (2C-*m*), 131.61 (2C-*o*), 124.06 (C-8), 121.26 (C-2b), 120.55 (C-11), 116.72 (C-7b), 115.59 (C-2c), 110.49 (C-13a), 105.02 (C-14a), 37.14 (C-14). MS m/z (%):502/504 (M^+ /M+2, 36/12), 490 (78), 432 (51), 249 (100), 194 (37). Anal. Calcd for $C_{25}H_{13}Cl_2N_5O_3$ (502.31): C, 59.78; H, 2.61; N, 13.94. Found: C, 59.97; H, 2.79; N, 14.30.

4.1.4.5. 9-bromo-14-(4-chlorophenyl)-2-(furan-2-yl)-12,14-dihydro-13H-[1,2,4]triazolo-[1'',5'':1',6']pyrimido[5',4':5,6]pyrano[3,2-c]quinolin-13-one (9e)

Yield: 0.390 g (79%); mp 261–263 °C, IR (KBr) υ_{max}/cm^{-1} 3321, 1650. ^{1}HNMR δ_H 12.07 (bs, 1H; NH), 10.14 (s, 1H; H-5), 9.00 (bs, 1H; H-8), 8.40 (d, *J* = 8.4, 1H; H-10), 8.23 (bs,1H; H-2d), 8.06 (d, *J* = 3.6, 1H; H-2b), 8.06 (d, *J* = 8.8, 1H; H-11), 7.89 (d, *J* = 8.1, 2H; H-*m*), 7.73 (d, *J* = 8.0, 2H; H-*o*), 7.21 (dd, *J* = 3.5, 1.5, 1H; H-2c), 6.51 (s, 1H; H-14). ^{13}CNMR δ_C 164.33 (C-13), 159.95 (C-6a), 156.54 (C-7a), 154.15 (C-2), 151.01 (C-2d), 150.55 (C-14b), 143.77 (C-5), 140.08 (C-2a), 139.43 (C-10), 138.70 (C-*p*), 138.18 (C-*i*), 137.32 (C-11a), 131.94 (2C-*m*), 131.61 (2C-*o*), 127.29 (C-8), 121.99 (C-9), 121.28 (C-2b), 120.55 (C-11), 117.02 (C-7b), 115.60 (C-2c), 110.50 (C-13a), 105.04 (C-14a), 37.16 (C-14). MS m/z (%): 546/548 (M^+ /M+2, 69/67), 505 (78), 460 (100), 394 (36). Anal. Calcd for $C_{25}H_{13}BrClN_5O_3$ (546.77): C, 54.92; H, 2.40; N, 12.81. Found: C, 54.65; H, 2.80; N, 12.50.

4.2. Biological evaluation

4.2.1. Screening of antiproliferative activity by NCI.

The methodology of the NCI procedure for primary anticancer assay was detailed on their site (http://www.dtp.nci.nih.gov). Briefly, the protocol was performed at sixty human cancer cell lines panel derived from nine different neoplastic diseases [35, 36]. NCI-60 testing is performed in a single dose of 10^{-5} M or 15 μg/mL concentration in all 60 cell lines in accordance with the protocol of the Drug Evaluation Branch, National Cancer Institute, Bethesda, USA.

4.2.2. Cytotoxic activity using MTT Assay and evaluation of IC_{50}

4.2.2.1. MTT assay

MTT assay was performed to investigate the effect of the synthesized compounds on the viability of mammary epithelial cells (MCF-10A) [37, 38]. **See Appendix A**

4.2.2.2. Assay for antiproliferative effect

To explore the antiproliferative potential of compounds MTT assay was performed according to previously reported procedure [39, 40] using different cell lines. **See Appendix A**

4.2.3. Caspase-3, 8 and 9 activation assays

Cell line cells of human Panc-1 pancreatic cell line were obtained from ATCC. RPMI 1640 containing 10% FBS was used to allow cells to grow at 37 ^{o}C, stimulated with the compounds to be tested for caspase 3, 8 and 9 [54, 55]. **See Appendix A**

4.2.4. Evaluation of Bax and Bcl-2 expressions

m RNA isolation was carried out using RNeasy extraction kit, up to 1 X 10^7 cells. They were disrupted in Buffer RLT and homogenized [56]. **See Appendix A**

4.2.5. Cell Apoptosis Assay

Apoptosis was determined by flow cytometry based on the annexin-V-fluoresce in isothiocyanate (FITC) and propidium iodide (PI) staining kit (BD Pharmingen, San Diego, USA) [57]. **See Appendix A**

4.2.6. p53 transcription in MCF-7

The transcription effects of 5a and 5b on p53 as a possible plausible mechanism for their anticancer efficacy have been evaluated and compared to reference doxorubicin [58]. **See Appendix A**

Acknowledgement

The NMR spectrometer at Florida Institute of Technology was purchased with the assistance of the U.S. National Science Foundation (CHE 03 41225).

References

1. Akhtar M. J.; Yar M. S.; Khan A. A.; Ali Z.; Haider M. R., Recent advances in the synthesis and anticancer activity of some molecules other than nitrogen containing heterocyclic moieties, *Mini Rev. Med. Chem*., **2017**, 17, 1602-1632.

2. Lee H.-Y.; Chang C.-Y.; Su C.-J.; Huang H.-L.; Mehndiratta S.; Chao Y.-H.; Hsu C.-M.; Kumar S.; Sung T.-Y.; Huang Y.-Z.; Li, Y.-H.; Yang C.-R.; Liou J.-P., 2-(Phenylsulfonyl)quinoline N-hydroxyacrylamides as potent anticancer agents inhibiting histone deacetylase, *Eur. J. Med. Chem*., **2016**, 122, 92-101.

3. Arafa R. K; Hegazy G. H.; Piazza G. A.; Abadi A. H., Synthesis and in vitro antiproliferative effect of novel quinoline-based anticancer agents, *Eur. J. Med. Chem*., **2013**, 63, 826-832.

4. Afzal O.; Kumar S.; Haider M. R.; Ali M. R.; Kumar R.; Jaggi M.; Bawa S., A review on anticancer potential of bioactive heterocycle quinoline, *Eur. J. Med. Chem.*, **2015**, 97, 871-910.

5. Wabo H. K.; Tane P.; Connolly J. D.; Okunji C. C.; Schuster B.; Iwu M. M., Tabouensinium chloride, a novel quaternary pyranoquinoline alkaloid from Araliopsis tabouensis, *Nat. Prod. Res.*, **2005**, 19, 591–595.

6. Chen I.-S.; Tsai I.-L.; Teng C.-M.; Chen J.-J.; Chang Y.-L.; Ko F.-N.; Lu M. C.; Pezzuto J. M., Pyranoquinoline alkaloids from Zanthoxylum simulans, *Phytochemistry,* **1997**, 46, 525–529.

7. Ramesh M.; Mohan P. A.; Shanmugam P., A convenient synthesis of flindersine, atanine and their analogues, *Tetrahedron*, **1984**, 40, 4041–4049.

8. Siliveri S.; Radhika T.; Babu V. H.; Raj S.; Reddy B. M., Synthesis and biological evaluation of pyrano[3,2-*h*]quinoline carbonitriles, *Int. J. Green Pharm.,* **2017**, 11, 423–429.

9. Magesh C. J.; Makesh S. V; Perumal P. T., Highly diastereoselective inverse electron demand (IED) Diels–Alder reaction mediated by chiral salen–AlCl complex: the first, target-oriented synthesis of pyranoquinolines as potential antibacterial agents, *Bioorg. Med. Chem. Lett.*, **2004**, 14, 2035–2040.

10. Martinez-Grau A.; Marco J. L., Friedländer reaction on 2-amino-3-cyano-4*H*-pyrans: synthesis of derivatives of 4*H*-pyrano[2, 3-*b*]quinoline, new tacrine analogues, *Bioorg. Med. Chem. Lett.* **1997**, 7, 3165–3170.

11. Kamperdick C.; Phuong N. M.; Van Sung T.; Adam G., Bisquinolinone alkaloids from Melicope pteleifolia, *Phytochemistry*, **1999**, 50, 177–181.

12. Chen J.-J.; Chen P.-H.; Liao C.-H.; Huang S.-Y.; Chen I.-S., New phenylpropenoids, bis(1-phenylethyl) phenols, bisquinolinone alkaloid, and anti-inflammatory constituents from Zanthoxylum integrifoliolum, *J. Nat. Prod*., **2007**, 70, 1444–1448.

13. Isaka M.; Tanticharoen M.; Kongsaeree P.; Thebtaranonth Y., Structures of cordypyridones A−D, antimalarial *N*-hydroxy- and *N*-methoxy-2-pyridones from the insect pathogenic fungus Cordyceps nipponica, *J. Org. Chem*., **2001**, 66, 4803–4808.

14. Koizumi F.; Fukumitsu N.; Zhao J.; Chanklan R.; Miyakawa T.; Kawahara S.; Iwamoto S.; Suzuki M.; Kakita S.; Rahayu E. S.; Hosokawa S.; Tatsuta K., Ichimura M. YCM1008A, a

novel Ca^{2+}-signalling inhibitor, produced by Fusarium sp. YCM1008, *J. Antibiot*., **2007**, 60, 455–458.

15. Fouda A. M., Halogenated 2-amino-4*H*-pyrano[3,2-*h*]quinoline-3-carbonitriles as antitumor agents and structure-activity relationships of the 4-, 6-, and 9-positions, *Med. Chem. Res*., **2017**, 26, 302–313.

16. Hammouda M. A. A.; El-Hag F. A. A.; El-Serwy W. S.; El-Manawaty M. A., Synthesis and characterization of new fused 4H-pyranoquinoline carbonitrile derivatives with anticipated antitumor biological activity, *Res. J. Pharm. Biol. Chem. Sci.*, **2015**, 6, 200–208.

17. Al-Ghamdi A. M.; El-Wahab A. H. F. A.; Mohamed H. M.; El-Agrody A. M., Synthesis and antitumor activities of 4H-pyrano[3,2-*h*]quinoline-3-carbonitrile, 7H-pyrimido[4′,5′:6,5]-pyrano[3,2-*h*]quinoline and 14H-pyrimido[4′,5′:6,5]pyrano[3,2-*h*][1,2,4]triazolo[1,5-*c*]-quinoline derivatives, *Lett. Drug Des. Discov.*, **2012**, 9, 459–470.

18. El-Agrody A. M.; Abd-Rabboh H. S. M.; Al-Ghamdi A. M., Synthesis, antitumor activity, and structure-activity relationship of some 4H-pyrano[3,2-*h*]quinoline and 7H-pyrimido[4′,5′:6,5]-pyrano[3,2-*h*]quinoline derivatives, *Med. Chem. Res*., **2013**, 22, 1339–1355.

19. Maalej E.; Chabchoub F.; Oset-Gasque M. J.; Esquivias-Pérez M.; González M. P.; Monjas L.; Pérez C.; de los Ríos C.; Rodríguez-Franco M. I.; Iriepa I.; Moraleda I.; Chioua M.; Romero A.; Marco-Contelles J.; Samadi A., Synthesis, biological assessment, and molecular modeling of racemic 7-aryl-9,10,11,12-tetrahydro-7*H*-benzo[7,8]chromeno[2,3-*b*]quinolin-8-amines as potential drugs for the treatment of Alzheimer's disease, *Eur. J. Med. Chem*., **2012**, 54, 750–763.

20. Nesterova I. N.; Alekseeva L. M.; Andreeva L. M.; Andreeva N. I.; Golovira S. M.; Granik V. G., Synthesis and pharmacological activity of derivatives of 5-dimethylaminopyrano-[3,2-c]quinolin-2-ones, *Pharm. Chem. J*., **1995**, 29, 111–114.

21. Lakomska I.; Fandzloch M., Application of 1,2,4-triazolo[1,5-a]pyrimidines for the design of coordination compounds with interesting structures and new biological properties, *Coord. Chem. Rev.,***2016**, 327–328, 221–241.

22. Majeed R.; Sangwan P. L.; Chinthakindi P. K.; Khan I.; Dangroo N. A.; Thota N.; Hamid A.; Sharma P. R.; Saxena A. K.; Koul S., Synthesis of 3-O-propargylated betulinic acid and its 1,2,3-triazoles as potential apoptotic agents, *Eur. J. Med. Chem*., **2013**, 63, 782–792.

23. Richardson C. M.; Williamson D. S.; Parratt M. J.; Borgognoni J.; Cansfield A. D.; Dokurno P.; Francis G. L.; Howes R.; Moore J. D.; Murray J. B.; Robertson A.; Surgenor A. E.; Torrance C. J., Triazolo[1,5-*a*]pyrimidines as novel CDK2 inhibitors: protein structure-guided design and SAR, *Bioorg. Med. Chem. Lett*., **2006**, 16, 1353–1357.

24. Zhai X.; Jiang N.; Zhang K. L.; Bao F.; Gong P., Design, synthesis and antiproliferative activity of novel 2,7-disubstituted triazolo[1,5-*a*]pyrimidines, *Chin. Chem. Lett*., **2009**, 20, 1179–1182.

25. Lakomska I.; Hoffmann K.; Wojtczak A.; Sitkowski J.; Maj E.; Wietrzyk J., Cytotoxic Malonate platinum(II) Complexes With 1,2,4-triazolo[1,5-*a*]pyrimidine Derivatives: Structural Characterization and Mechanism of the Suppression of Tumor Cell Growth, *J. Inorg. Biochem*. **2014**, 141, 188–197.

26. Lakomska I.; Hoffmann K.; Topolski A.; Kloskowski T.; Drewa T., Spectroscopic, kinetic and cytotoxic in vitro study of hexafluoroglutarate platinum(II) complex with 5,7-dimethyl-1,2,4-triazolo[1,5-*a*]pyrimidine, *Inorg. Chim. Acta*, **2012**, 387, 455–459.

27. Lauria A.; Abbate I.; Patella C.; Martorana A.; Dattolo G.; Almerico A. M., New annelated thieno[2,3-*e*][1,2,3]triazolo[1,5-*a*]pyrimidines, with potent anticancer activity, designed through VLAK protocol, *Eur. J. Med. Chem*., **2013**, 62, 416–424.

28. Kamal R.; Kumar V.; Kumar R.; Bhardwaj J. K.; Saraf P.; Kumari P.; Bhardwaj V., Design, synthesis, and screening of triazolopyrimidine–pyrazole hybrids as potent apoptotic inducers, *Arch. Pharm. Chem. Life Sci*., **2017**, 350, e1700137

29. El-Sheref E. M.; Aly A. A.; Mourad A.-F. E.; Brown A. B.; Bräse S.; Bakheet M. E. M., Synthesis of pyrano[3,2-*c*]quinoline-4-carboxylates and 2-(4-oxo-1,4-dihydroquinolin-3-yl)fumarates, *Chem. Pap.,* **2018**, 72, 181-190.

30. Aly A.A.; El-Sheref E.M.; Mourad A.-F. E, Brown A. B.; Bräse S.; Bakheet M. E. M, Nieger M., Synthesis of spiro(indoline-3,4'-pyrano[3,2-c]quinoline)-3'-carbonitriles, *Monatsh.Chem.,* **2018**, 149, 635–644.

31. Aly A. A.; Ishak, E. A.; Shawky A. M., Mohamed, A. H. Formation of furo[3,2-c]quinolone-2-carbonitriles and 4-oxo-4,5-dihydrofuro[3,2-*c*]quinolone-2-carboxamides from reaction of quinoline-2,4-diones with 2-[bis(methylthio)methylene] malononitrile, *Monatsh. Chem.,* **2020**, 151, 223–229.

32. Aly A. A.; El-Sheref E. M.; Bakheet M. E. M.; Mourad A.-F. E.; Bräse S.; Ibrahim M. A. A.; Nieger M.; Garvalov B. K.; Dalby K. N.; Kaoud T. S. Design, synthesis and biological evaluation of fused naphthofuro[3,2-*c*]quinoline-6,7,12-triones and pyrano[3,2-*c*]quinolone-6,7,8,13-tetraone derivatives as ERK inhibitors with efficacy in BRAF-mutant melanoma, *Bioorg. Chem.,* **2019**, 82, 290-305.

33. Aly A. A.; El-Sheref E. M.; Mourad A.-F. E.; Bakheet M. E. M.; Bräse S.; Nieger M. One-pot synthesis of 2,3-bis-(4-hydroxy-2-oxo-1,2-dihydroquinolin-3-yl)succinates and aryl methylene-bis-3,3'-quinoline-2-ones, *Chem Pap*., **2019**, 73, 27-37.

34. Aly A. A.; El-Sheref E. M.; Bakheet M. E. M.; Mourad M. A. E.; Brown A. B.; Bräse S.; Nieger M.; Ibrahim M. A. A. Synthesis of novel 1,2-bis-quinolinyl-1,4-naphthoquinones: ERK2 inhibition, cytotoxicity and molecular docking studies, *Bioorg. Chem.,* **2018**, 81, 700-712.

35. El-Sherief H. A. M.; Youssif B. G. M.; Bukhari S. N. A.; Abdel-Aziz M.; Abdel-Rahman H. M., Novel 1,2,4-triazole derivatives as potential anticancer agents: design, synthesis, molecular docking and mechanistic studies, *Bioorg. Chem*., **2018,** 76, 314-325.

36. El-Sherief H. A. M.; Youssif B. G. M.; Bukhari S. N. A.; Abdelazeem A. H.; Abdel-Aziz M.; Abdel-Rahman H. M., Synthesis, anticancer activity and molecular modelling studies of 1,2,4-triazole derivatives as EGFR inhibitors, *Eur. J. Med. Chem*., **2018**, 156, 774-789.

37. M. H. Abdelrahman, A. S. Aboraia, B. G. M. Youssif, B. E. M. Elsadek, Design, Synthesis and Pharmacophoric Model Building of New 3-Alkoxymethyl / 3-Phenyl indole-2-carboxamides with Potential Antiproliferative Activity, *Chem Biol Drug Des.,* **2017**, 90, 64-82.

38. B.G. Youssif, A.M. Mohamed, E.E.A. Osman, O.F. Abou-Ghadir, D.H. Elnaggar, M.H. Abdelrahman, L. Treamblu, H.A. Gomaa, 5-Chlorobenzofuran-2-carboxamides: From allosteric CB1 modulators to potential apoptotic antitumor agents, *Eur. J. Med. Chem*., **2019**, 177, 1-11.

39. A.H. Abdelazeem, M.T. El-Saadi, E.G. Said, B.G. Youssif, H.A. Omar, S.M. El-Moghazy, Novel diphenylthiazole derivatives with multi-target mechanism: Synthesis, docking study, anticancer and anti-inflammatory activities, *Bioorg. Chem*., **2017**, 75, 127-138.

40. M.S. Abdelbaset, G.E.-D.A. Abuo-Rahma, M.H. Abdelrahman, M. Ramadan, B.G. Youssif, S.N.A. Bukhari, M.F. Mohamed, M. Abdel-Aziz, Novel pyrrol-2(3H)-ones and pyridazin-3 (2H)-ones carrying quinoline scaffold as anti-proliferative tubulin polymerization inhibitors, *Bioorg. Chem*., **2018**, 80, 151-163.

41. Nguyen T.; Li J.-X.; Thomas B. F.; Wiley J. L.; Kenakin T. P.; Zhang Y., Allosteric modulation: an alternate approach targeting the cannabinoid CB1 receptor, *Med. Res. Rev.*, **2017**, 37, 441-474.

42. Cohen G. M., Caspases: the executioners of apoptosis*, Biochem. J*., **1997**, 326, 1-16.

43. Slee E. A.; Adrain C.; Martin S. J., Executioner caspase 3, -6, and -7 perform distinct, non-redundant roles during the demolition phase of apoptosis, *J. Biol. Chem*., **2001**, 276, 7320-7326.

44. Daina A.; Michielin O.; Zoete V., SwissADME: a free web tool to evaluate pharmacokinetics, drug-likeness, and medicinal chemistry friendliness of small molecules, *Sci. Rep.,* **2017**, 7, 42717.

45. Lipinski C. A; Lombardo F; Dominy B. W; Feeney P.J., Experimental and computational approaches to estimate solubility in drug discovery and development settings, *Adv. Drug Deliv. Rev*., **2001**, 46, 3-26.

46. Ghose A. K.; Viswanadhan V. N.; Wendoloski J. J., A knowledge-based approach in designing combinatorial or medicinal chemistry libraries for drug discovery. 1. A qualitative and quantitative characterization of known drug databases, *J. Comb. Chem*.,**1999**, 1, 55-68.

47. Veber D. F.; Johnson S. R.; Cheng H.-Y.; Smith B. R.; Ward K. W.; Kopple K. D., Molecular properties that influence the oral bioavailability of drug candidates, *J. Med. Chem.*, **2002**, 45, 2615-2623.

48. Egan W. J.; Merz K. M. Jr; Baldwin J. J., Prediction of drug absorption using multivariate statistics, *J. Med. Chem*., **2000**, 43, 3867-3877.

49. Muegge I.; Heald S. L.; Brittelli D., Simple selection criteria for drug-like chemical matter, *J. Med. Chem*., **2001**, 44, 1841-1846.

50. Baell J. B.; Holloway G. A., New substructure filters for removal of pan assay interference compounds (PAINS) from screening libraries and for their exclusion in bioassays*, J. Med. Chem.*, **2010**, 53, 2719-2740.

51. Rao V. S.; Darbarwar M. One pot synthesis of 7-[1,2-dihydro-4-hydroxy-1-methyl/phenyl-2-oxo-3-quinolinyl]-5,7-dihydro-5-methyl/phenyl-6*H*-[1]-benzo-pyrano-[3,2-*c*]quinolin-6-ones, *Synth. Commun.,* **1988**, 18, 2267-2272.

52. Buckle D. R.; Cantello B. C. C.; Smith H.; Spicer B. A. 4-Hydroxy-3-nitro-2-quinolones and related compounds as inhibitors of allergic reactions, *J. Med. Chem.* **1975**, 18, 726-732.

53. Elinson M. N.; Nasybullin R. F.; Nikishin G. I., Electrocatalytic fast and efficient multicomponent approach to medicinally relevant pyrano[3,2-*c*]quinolone scaffold, *J. Electrochem. Soc*., **2013**, 160, G3053-G3057.

54. Abou-Zied H. A.; Youssif B. G. M.; Mohamed M. F. A.; Hayallah A. M.; Abdel-Aziz M., EGFR inhibitors and apoptotic inducers: Design, synthesis, anticancer activity and docking studies of novel xanthine derivatives carrying chalcone moiety as hybrid molecules, *Bioorg. Chem*., **2019**, 89, 102997.

55. Hisham M.; Youssif B. G. M.; Osman E. E. A.; Hayallah A. M.; Abdel-Aziz M., Synthesis and biological evaluation of novel xanthine derivatives as potential apoptotic antitumor agents, *Eur. J. Med. Chem*., **2019**, 176, 117-128.

56. Elbastawesy M. A. I.; Aly A. A.; Ramadan M.; Elshaier Y. A. M. M.; Youssif B. G. M.; Brown A. B.; Abuo-Rahma G. E-D. A., Novel pyrazoloquinolin-2-ones: design, synthesis, docking studies, and biological evaluation as antiproliferative EGFR-TK inhibitors; *Bioorg. Chem*., **2019**, 90, 103045.

57. B. G. M. Youssif, M. H. Abdelrahman, A. H. Abdelazeem, M. A. abdelgawad, H. M. Ibrahim, O. I. A. Salem, M. F. A. Mohamed, L. Treamblu, S. N. A. Bukhari, Design, synthesis, mechanistic and histopathological studies of small-molecules of novel indole-2-carboxamides and pyrazino[1,2-*a*]indol-1(2*H*)-ones as potential anticancer agents effecting the reactive oxygen species production, *Eur. J. Med. Chem*., **2018**, 146, 260-273.

58. P.H. Shaw, The role of p53 in cell cycle regulation, Pathol. Res. and Pract., **1996,** 192, 669-675.

Appendix A

3. Experimental

General Details

Melting points were determined using open glass capillaries on a Gallenkamp melting point apparatus (Weiss–Gallenkamp, Loughborough, UK) and are uncorrected. The IR spectra were recorded from potassium bromide disks with a FT device; Minia University NMR spectra were measured in DMSO-*d6* on a Bruker AV-400 spectrometer (400 MHz for ^{1}H, 100 MHz for ^{13}C, and 40.55 MHz for ^{15}N); chemical shifts are expressed in δ (ppm), versus internal Tetramethylsilane (TMS) = 0 for ^{1}H and ^{13}C, and external liquid ammonia = 0 for ^{15}N. Coupling constants, as stated in Hz. Correlations were established using ^{1}H–^{1}H COSY, and ^{1}H–^{13}C and ^{1}H–^{15}N HSQC and HMBC experiments. Mass spectra were recorded on a Finnigan Fab 70 eV, Institute of Organic Chemistry, Karlsruhe Institute of Technology, Karlsruhe, Germany. TLC was performed on analytical Merck 9385 silica aluminium sheets (Kieselgel 60) with Pf_{254} indicator; TLCs were viewed at λmax = 254 nm. Elemental analyses were carried out at the Microanalytical Centre, Cairo University, Egypt. Trimethyl orthoformate, triethyl orthoformate**,** acetohydrazide and furan-2-carbohydrazide were obtained from commercial source and used as received.

Biological Evaluation

The NCI-60 anticancer drug screen

The methodology of the NCI [31, 32] for primary anticancer assay was performed at sixty human tumor cell lines panel derived from nine neoplastic diseases, in accordance with the protocol of the Drug Evaluation Branch, National Cancer Institute, Bethesda. Tested compounds were added to the culture at a single concentration (10^{-5} M) and the cultures were incubated for 48 h. End point determinations were made with a protein binding dye, Sulforhodamine B (SRB). Results for each tested compound were reported as the percentage of growth of the treated cells when compared to the untreated control cells. The percentage of growth was evaluated spectrophotometrically versus controls not treated with test agents. the cytotoxic and/or growth inhibitory effects of the tested compound was tested *in vitro* against the full panel of 60 human tumor cell lines derived from nine neoplastic diseases at 10-fold dilutions of five concentrations ranging from 10^{-4} M to 10^{-8} M. Three doses response parameter were calculated for each cell line, GI_{50}, TGI and LC_{50}.

MTT assay

MTT assay was performed to investigate the effect of the synthesized compounds on mammary epithelial cells (MCF-10A). The cells were propagated in medium consisting of Ham's F-12 medium/Dulbecco's modified Eagle's medium (DMEM) (1:1) supplemented with 10% foetal calf serum, 2 mM glutamine, insulin (10 µg/mL), hydrocortisone (500 ng/mL) and epidermal growth factor (20 ng/mL). Trypsin ethylenediamine tetra acetic acid (EDTA) was used to passage the cells after every 2–3 days. 96-well flat-bottomed cell culture plates were used to seed the cells at a density of 10^4 cells mL^{-1}. The medium was aspirated from all the wells of culture plates after 24 h followed by the addition of synthesized compounds (in 200 µL medium to yield a final concentration of 0.1% (v/v) dimethylsulfoxide) into individual wells of the plates. Four wells were designated to a single compound. The plates were allowed to incubate at 37 ^oC for 96 h. Afterwards, the medium was aspirated and 3-[4,5-dimethylthiazol-2-yl]-2,5-

diphenyltetrazolium bromide (MTT) (0.4 mg/mL) in medium was added to each well and subsequently incubated for 3 hr. The medium was aspirated and 150 µL dimethyl sulfoxide (DMSO) was added to each well. The plates were vortexed followed by the measurement of absorbance at 540 nm on a micro plate reader. The results were presented as inhibition (%) of proliferation in contrast to controls comprising 0.1% DMSO.

Antiproliferative Assay

Propidium iodide fluorescence assay was carried out on Panc-1(pancreas cancer), PaCa-2 (pancreatic carcinoma), MCF-7 (breast cancer): A-549 (epithelial): HT-29 (colon cancer), H-460 (lung cancer) and PC-3 (prostate cancer) cell lines to investigate the antiproliferative activity of compounds(....). Propidium iodide is a fluorescence dye which possesses ability to attach with DNA, therefore providing a precise and quick method for the calculation of total nuclear DNA. PI is incapable of crossing the plasma membrane and its fluorescence signal intensity is directly proportional to the amount of cellular DNA. Thus, cells with damaged plasma membranes or altered permeability are totaled as dead ones. To perform the assay, cells were seeded in 96-well flat-bottomed culture plates at a density of 3000–7500 cells/well in 200 µL medium and incubated at 37 ^{o}C for 24 h in humidified 5% CO_2/95% air atmosphere. Later, the compounds at 10 µM concentrations (in 0.1% DMSO) were added in triplicate wells while 0.1% DMSO served as control, followed by a 48-h incubation of plates. The medium was removed and 25 µL PI (50 µg/mL in water/medium) was added in each well. The plates were then frozen at -80 ^{o}C for 24 h, followed by thawing and equilibration to 25 LC. The readings were recorded at excitation and emission wavelengths of 530 and 620 nm using a fluorometer (Polar-Star BMG Tech). Following formula was used to calculate the cytotoxicity (%) of compounds:

% cytotoxicity = A_c-A_{Tc} / A_c * 100

Where A_C = Absorbance of control and A_{TC} = Absorbance of treated cells. To equate the results, Doxrubicin was used as positive control.

4.2.3. Caspase-3, 8 and 9 activation assays

Cell line cell of Panc-1 was obtained from ATCC. RPMI 1640 containing 10% FBS was used to allow cells to grow at 37 ^oC, stimulated with the compounds to be tested for caspase-3, caspase-8 and caspase-9, and lysed with Cell Extraction Buffer. Standard Diluent Buffer was used to dilute the lysate over the range of the assay and measure human active caspase-3, caspase-8 and caspase-9 content. (cells are Plated in a density of 1.2-1.8 X 10,000 cells/well in a volume of 100 lL complete growth medium + 100 lL of the tested compound per well in a 96-well plate for 24/48 h before the enzyme assay) [45, 46].

4.2.4. Evaluation of Bax and Bcl-2 expressions

m RNA isolation was carried out using RNeasy extraction kit, up to 1 X 10^7 cells. They were disrupted in Buffer RLT and homogenized. To promote selective binding of RNA to the RNeasy membrane, ethanol was added to the lysate. Then, the sample was applied to the RNeasy Mini spin column. Total RNA bound to the membrane. Using RNase-free water, high quality of RNA was eluted. A micro-centrifuge was used to centrifuge all binds, wash, and elution steps [47].

Kit contents was BIORAD iScriptTM One-Step Real-Time RT-PCR Kit with SYBR@ Green. Reagent used is described as following: iScript Reverse Transcriptase Optimized 50X formulation of iScript MMLV for One-Step RT-PCR reverse transcriptase for One-Step RTPCR procedures (yellow cap) 2X SYBR_ Green RT-PCR 2X reaction buffer containing 0.4 mM of each dNTP (dATP, Reaction Mix dCTP, dGTP, dTTP), magnesium chloride, iTaq DNA (green cap) polymerase, 20 nM fluorescein, SYBR_ Green I dye, stabilizers Nuclease-free H_2O. A reaction mix (50 lL) was prepared according to the following recipe: 2X Sybr Green

RT-PCR Master (25 lL), (10 lM) forward primer (1.5 10 lL), (10 lM) Reverse primer (1.5 lL), Nuclease-free H2O (11 lL), RNA template (1 pg to 100 ng total RNA) (10 lL) and iScript Reverse Transcriptase for One-Step RT-PCR (1 lL). Amplification was performed using 7500 Fast RT-PCR Systems (Applied Biosystems, USA) 10 ng of cDNA using a Power Sybr Green PCR Master MIX (Applied Biosystems) [46]. The amplification protocol was as follows: cDNA synthesis: 50 ^{o}C (10 min), iScript Reverse transcriptase inactivation: 95 ^{o}C (5 min), PCR cycling and detection (40 cycle): 95 ^{o}C (10 s), data collection step: 60 ^{o}C (30 s), melt curve analysis: 95 ^{o}C (1 min), 55 ^{o}C (1 min) and 55 ^{o}C (10 s) (80 cycles, increasing each by 0.5 ^{o}C each cycle). Then the products were routinely checked using dissociation curve software. Transcript quantities were compared by the relative Ct method and the amount of BAX and BCL2 were normalized to the endogenous control (GAPDH). By 2-DDCT, the value in relation to the control sample was given and real-time PCR primer sequences were as the following:

Bax F 50-GTTTCA TCC AGG ATC GAG CAG-30

Bax R 50-CATCTT CTT CCA GAT GGT GA-30

Bcl-2 F 50-CCTGTG GAC TGA GTA CC-30

Bcl-2 R 50-GAGACA GCC AGG AGA AAT CA-30

To evaluate any problem related to primer unspecific annealing or any secondary structure formation, a dissociation assay was performed. Data was analyzed using SDS Analysis Software.

Cell cycle analysis and apoptosis assay [48, 49]

Cell cycle analysis and apoptosis detection.

Cell cycle analysis was performed for compound **5a** on MCF-7 cell line. After treatment, the cells were suspended in 0.5 mL of PBS, collected by centrifugation, and fixed in ice-cold 70% (v/v) ethanol washed with PBS, resuspended with 0.1 mg/mL RNase, stained with 40 mg/ml

PI, and analyzed by flow cytometry using FACS caliber (Becton Dickinson). The cell cycle distributions were calculated using Phoenix Flow Systems and Verity Software House

Apoptosis assay

The MCF-7 was treated with IC_{50} of compound **5a** for 24 h. After treatment, the cells were suspended in 0.5 mL of PBS, collected by centrifugation, and fixed in ice-cold 70% (v/v) ethanol, centrifuged the ethanol-suspended cells for 5 min, suspended in 5 mL PBS and centrifuged for 5 min, re-suspended with 1 mL PI staining solution (0.1 mg/ml RNase) + PE Annexin V (component no. 51-65875X) and kept in dark at 37 ˚C for 10 min, finally analyzed by flow cytometry using FACS caliber (Becton Dickinson). The cell cycle distributions were calculated using Phoenix Flow Systems and Verity Software House.

p53 transcription in MCF-7

Firstly, total RNA was extracted according to RNA Spin Mini RNA isolation Kit (GE Healthcare lot. no # 1510/001) from MCF7 cell lines that treated with **5a** and **5b** and also from non-treated MCF7 cells as a negative control, then the extracted RNA was measured to evaluate its purity by using UV spectroscopy and to determine its concentration by using Nano drop. In addition, the extracted RNA was electrophoresed on 1.2% Formaldehyde agarose gel at 5–8 volt/cm to estimate the integrity of our extract. Secondary, first c-DNA strand was synthesized as follow: 2 ml from each primer (forward and reverse primers) for p53 gene was added into11 ml DEPC water, 8 ml 5X RNA buffer, 1 ml RNAase inhibitor, 4 ml dNTP mixture, and finally 2 ml MMUL reverse transcriptase (Fermentas, Revert Aid, # EP0441) was added. All the contents were then mixed well and incubated for 2 h in thermal cycle at (42 ^{0}C) before entering the qPCR. Then the following mixture [25 ml master mix, 3 ml forward primer, 3 ml reverse primer, 9 ml nuclease free water, 5 ml cDNA] was prepared for each gene and incubated in thermal gradient cycle for 35 cycle (6 h), using temperature range from (53 ^{0}C to 63 ^{0}C). After

that, the PCR products were run on 1.5% agarose gel to determine the best annealing temperature for each gene [58].

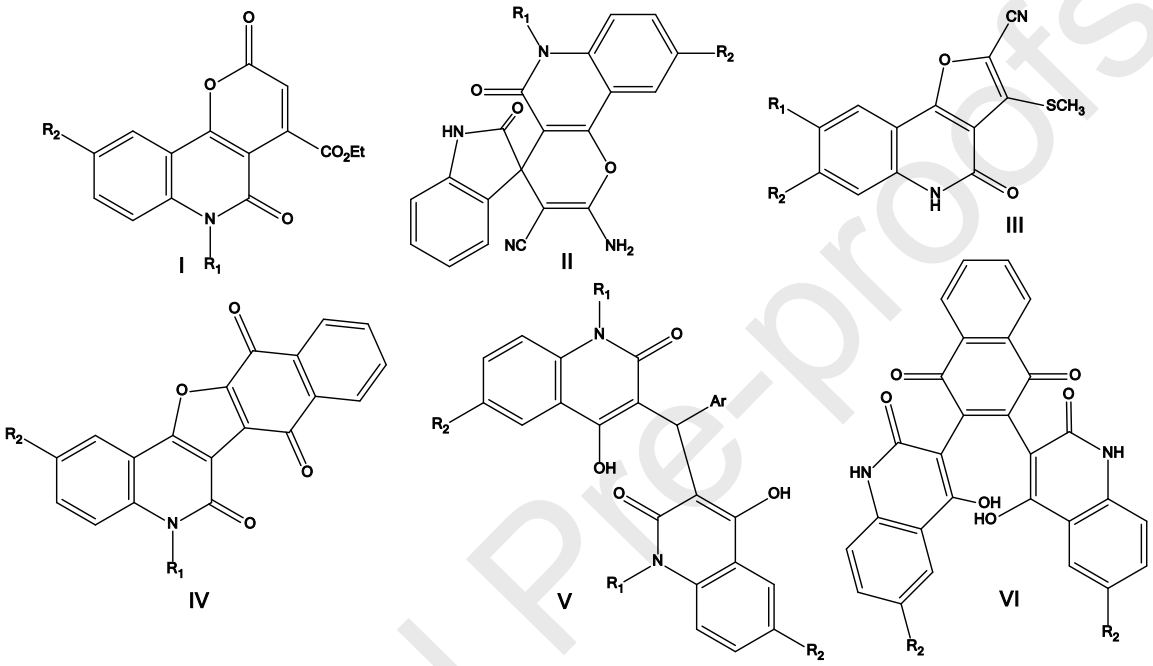

Figure 1. Chemical structure of some previously reported Quinolones **I-VI**

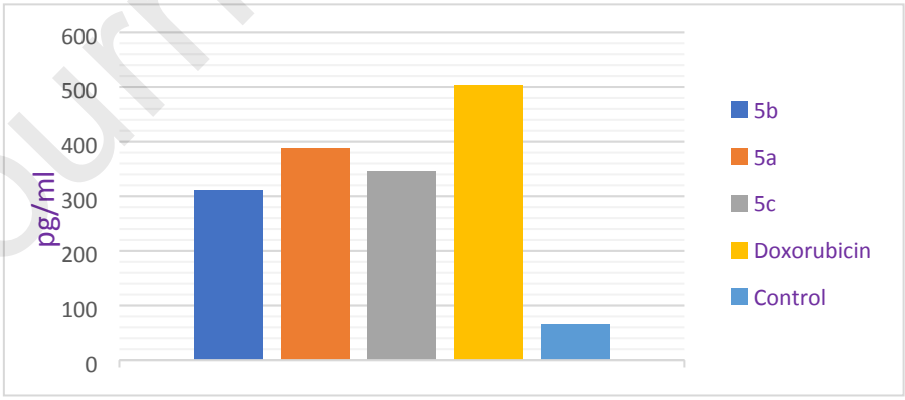

Figure 2. Caspase-3 level for compounds **5a-c** and **doxorubicin** in human breast cancer cell line (MCF-7)

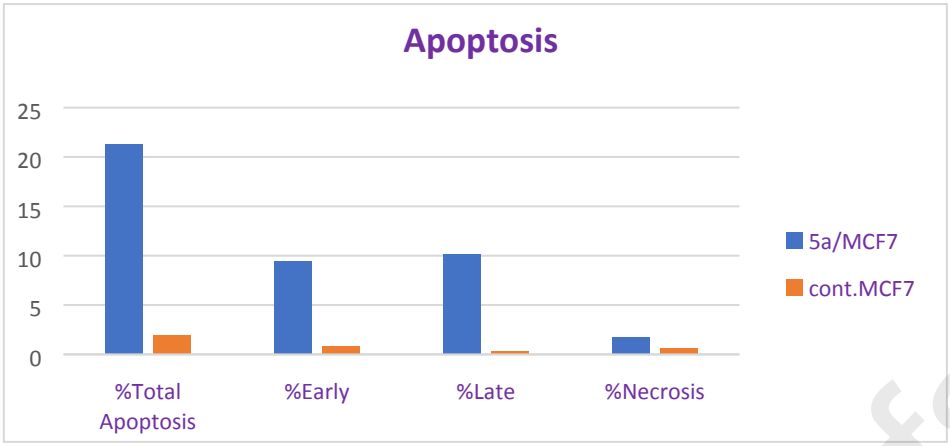

Figure 3. Apoptosis induction analysis using Annexin V/PI for compound **5a**

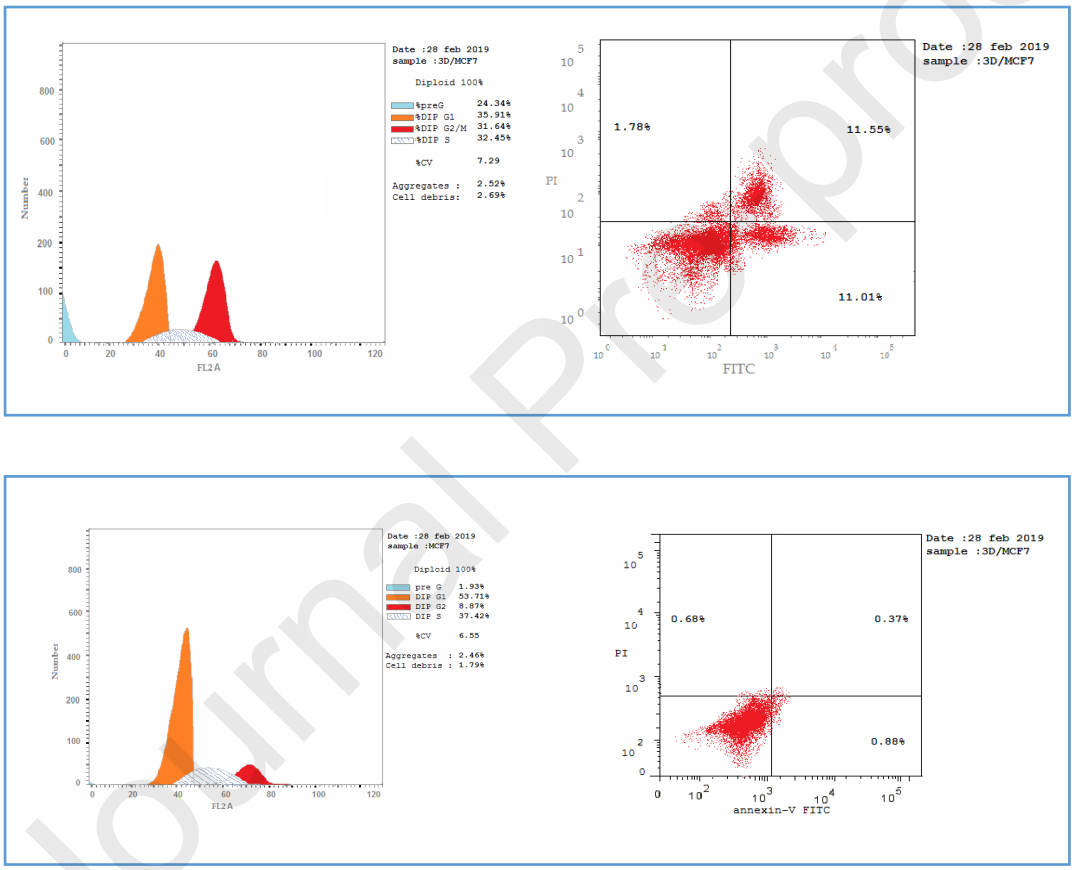

Figure 4. Cell cycle analysis and Apoptosis induction analysis of compound **5a** on MCF-7.

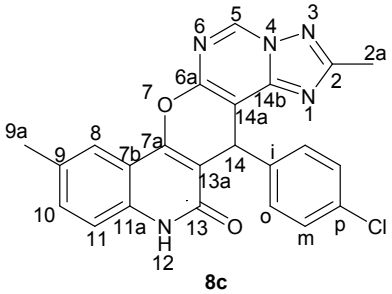

8c

Table 1. NMR spectroscopic assignments of compound **8c**

^{1}HNMR (DMSO-d_6)	**COSY**	**Assignment**
12.05 (s; 1H)		NH-12
10.08 (bs; 1H)		H-5
8.73 (d, J = 1.6; 1H)	*8.24, 3.09*	H-8
8.24 (d, J = 8.2; 1H)	*8.73,* 8.07	H-10
8.07 (d, J = 8.5; 1H)	8.24	H-11
7.85 (d, J = 7.9; 2H)	7.74	H-m
7.74 (d, J = 7.8; 2H)	7.85	H-o
6.44 (s; 1H)		H-14
3.22 (s; 3H)		H-2a
3.09 (s; 3H)	*8.73*	H-9a

^{13}C NMR (DMSO-d_6)	**HSQC:**	**HMBC:**	**Assignment**
164.0		6.38, 4.33	C-13
161.75		3.22	C-2
160.49		10.08, 6.44	C-6a
158.17		8.73, *8.07, 6.44*	C-7a
149.73		10.08	C-14b
144.02	10.08	10.08	C-5
141.11		8.07, 3.09	C-9
138.72	8.24	8.73, 7.85, 7.74	C-10
138.58		8.73, 7.74	C-*i*
137.58		8.73, 7.74	C-*p*
136.72		8.73, 8.24, *6.44*	C-11a
132.04	7.85	7.85, 6.44	C-*m*
131.88	7.74	7.74, 6.44	C-*o*
123.96	8.73	8.24,3.09	C-8
119.47	8.07		C-11
116.26		8.07	C-7b
107.17		6.44	C-13a
104.61		10.08, 6.44	C-14a
37.39	6.44	7.85	C-14
21.90	3.09	8.73, 8.24, 3.09	C-9a
12.59	3.22	3.22	C-2a

^{15}NNMR (DMSO-d_6)	**HSQC**	**HMBC:**	**Assignment**
263.5		3.22	N-3
243.9		10.08	N-6
226.0		10.08	N-4
149.6		3.22	N-1
147.4		8.07	N-12

Table 2: Percentage growth inhibition (GI %) of *in vitro* subpanel tumor cell lines at 10 μM concentration for compounds **5a-e**, **8a-e**, and **9a-e**.

Subpanel cancer cell Lines	% Growth Inhibition (GI %) [a]														
	5a	**5b**	**5c**	**5d**	**5e**	**8a**	**8b**	**8c**	**8d**	**8e**	**9a**	**9b**	**9c**	**9d**	**9e**
Leukemia															
CCRF-CEM	33.12	26.12	15.24	15.95	12.74	23.80	-	-	-	-	-	-	13.45	-	-
HL-60(TB)	46.57	27.34	18.27	18.31	11.36	33.79	-	17.70	-	-	10.10	-	13.65	-	-
K-562	**80.38**	20.04	22.10	19.25	11.90	21.50	-	15.64	-	-	8.44	-	11.07	-	-
MOLT-4	24.81	11.92	-	11.30	-	24.14	-	-	-	-	-	-	-	-	-
RPMI-8226	11.90	41.62	35.12	33.79	69.81	48.89	13.79	30.74	-	-	-	-	-	-	13.89
SR	**77.26**	37.74	19.07	25.22	13.32	16.65	-	-	-	-	-	-	31.47	-	-
Non-small cell lung cancer															
A549/ATCC	36.35	25.15	10.05	-	-	13.62	-	-	-	-	-	-	-	-	-
EKVX	26.02	51.18	18.04	18.32	30.46	22.72	13.90	21.29	11.84	-	9.01	-	14.54	-	-
HOP-62	35.37	50.04	25.26	19.40	29.26	15.39	12.72	13.67	-	-	2.21	-	-	-	-
HOP-92	20.83	62.30	38.58	38.91	49.25	48.91	25.85	34.83	-	-	12.06	21.53	29.77	-	31.91
NCI-H226	-	34.54	15.58	18.36	21.07	13.11	-	-	-	-	-	-	-	-	-
NCI-H23	19.67	23.92	13.70	12.90	14.63	-	-	-	-	-	-	-	-	-	-
NCI-H322M	14.08	24.70	-	-	12.01	-	-	-	-	-	-	-	-	-	-
NCI-H460	20.12	14.92	-	-	-	-	-	-	-	-	-	-	-	-	-
NCI-H522	41.29	30.65	27.90	21.49	25.84	24.06	12.40	16.94	-	-	-	-	16.00	24.84	-
Colon cancer															
COLO 205	-	-	-	-	-	12.36	-	-	-	-	-	-	-	-	-
HCC-2998	-	13.44	-	-	-	-	-	-	-	-	-	-	-	-	-
HCT-116	18.35	32.49	11.18	-	17.59	16.05	11.18	15.12	-	-	11.12	-	-	-	-
HCT-15	16.13	35.05	-	-	-	14.16	-	-	-	-	-	-	-	-	-
HT29	25.49	27.02	-	-	19.50	13.66	-	-	-	-	-	-	-	-	-
KM12	-	-	-	-	-	-	-	-	-	-	-	-	-	-	-
SW-620	16.61	26.37	-	-	15.40	-	-	-	-	-	-	-	-	-	-
CNS cancer															
SF-268	20.19	25.67	14.31	-	-	16.67	14.31	15..06	-	11.6	-	-	11.68	-	-
SF-295	23.11	12.07	-	-	-	-	-	-	-	-	-	-	-	-	-
SF-539	13.62	34.54	-	-	24.08	16.41	-	13.43	-	-	-	-	-	-	-
SNB-19	13.62	24.20	-	11.79	15.26	20.47	-	22.73	-	13.5	-	-	13.58	-	-
U251	12.61	19.18	-	-	-	18.06	-	-	-	-	-	-	-	-	-
Melanoma															
LOX IMVI	12.60	23.26	-	-	13.17	-	-	11.02	-	-	-	-	-	-	-
MALME-3	14.18	22.51	-	-	18.24	16.08	-	12.02	-	-	-	-	-	-	-
M14	-	25.06	-	-	12.90	-	-	-	-	-	-	-	-	-	-
MDA-MB-435	-	14.84	-	-	-	-	-	-	-	-	-	-	-	-	-

SK-MEL-2	-	10.92	-	-	-	-	-	-	-	-	-	-	-	-	-
SK-MEL-28	-	-	-	-	-	-	-	-	-	-	-	-	-	-	-
SK-MEL-5	11.56	32.63	-	-	12.85	14.78	-	-	-	-	-	-	-	-	-
UACC-257	-	-	-	-	-	-	-	-	-	-	-	-	-	-	-
UACC-62	26.81	40.22	-	-	53.55	-	-	29.66	24.88	-	-	-	-	-	-
Ovarian cancer															
IGROV1	26.57	55.97	-	-	40.94	-	-	18.44	26.18	-	11.27	-	-	-	-
OVCAR-3	-	18.31	-	-	35.75	-	-	-	-	-	-	-	-	-	-
OVCAR-4	24.74	32.47	-	-	31.36	-	-	28.24	20.09	-	2.43	-	16.17	-	-
OVCAR-5	12.54	26.40	-	-	14.85	-	-	-	11.15	-	-	-	13.17	-	-
OVCAR-8	-	20.69	-	-	13.69	-	-	-	-	-	3.12	-	-	-	-
NCI/ADR-RES	-	11.79	-	-	42.71	-	-	14.80	-	-	-	-	-	-	-
SK-OV-3	-	40.16	-	19.52	18.22	-	-	-	11.48	-	-	-	-	-	-
Renal cancer															
A498	34.06	40.39	-	-	52.06	-	-	13.54	44.14	-	-	-	-	-	-
ACHN	13.66	34.57	-	-	24.27	-	-	12.36	14.70	-	-	-	-	-	-
CAKI-1	41.76	53.67	16.16	-	100.28	-	16.16	25.90	30.78	-	42.23	-	24.51	-	-
RXF 393	25.39	40.89	-	-	43.17	-	-	26.55	12.64	-	-	-	-	-	-
SN12C	16.72	25.37	-	-	25.37	-	-	19.90	20.64	-	22.14	-	-	-	-
TK-10	-	-	-	-	-	-	-	-	-	-	-	-	-	-	-
UO-31	36.13	65	35.49	15.14	45.81	20.92	35.49	37.11	39.27	-	33.15	15.14	-	-	-
Prostate cancer															
PC-3	13.77	27.89	16.64	-	42.25	-	16.64	24.23	15.16	-	16.84	-	11.79	-	-
DU-145	-	-	-	-	-	-	-	-	-	-	-	-	-	-	-
Breast cancer															
MCF7	58.30	31.29	-	13.34	8.01	-	-	15.74	19.74	-	13.23	15.38	-	-	-
MDA-MB-231/ATCC	48.75	51.24	12.11	-	21.69	-	12.11	28.67	29.26	-	22.45	-	17.61	-	-
HS 578T	34.77	**64.39**	-	-	2.87	-	-	-	34	-	-	-	-	-	-
BT-549	18.64	23.12	152.73	-	4.72	-	152.73	-	15.06	-	14.23	-	-	-	11.83
T-47D	34.91	39.11	13.97	-	10.40	-	13.97	24.47	26.35	-	15.22	10.76	-	-	-
MDA-MB-468	46.02	14.08	-	-	3.08	-	-	-	-	-	-	-	-	-	-

(–): Weak activity GI <10%.

Table 3. Antiproliferative activity of compounds **5a-e, 8a-e** and **9a-e** and **Doxorubicin**

Comp.	Cell viability %	Antiproliferative activity IC_{50}± SEM (µM)				
		A-549	MCF-7	Panc-1	HT-29	Average (IC_{50})
5a	**91**	2.9±0.5	2.2±0.08	3.1±0.2	3.2±0.2	2.850
5b	**84**	4.7±0.4	4.3±0.8	4.6±0.6	4.7±0.4	4.575
5c	**86**	7.7±0.4	7.9±0.6	7.6±0.8	7.9±0.8	7.775
5d	**89**	10.9±0.8	10.5±1.1	10.6±0.8	10.4±1.2	10.60
5e	**85**	8.8±3.2	8.5±2.7	8.7±3.1	8.2±3.4	8.300
8a	**87**	30.4±3.2	30.5±2.7	30.7±3.1	31.2±3.4	30.700
8b	**82**	19.2±1.5	18.9±1.2	19.2±2.2	19.8±2.4	19.275
8c	**90**	15.7±2.5	15.6±2.9	15.8±1.9	15.8±1.6	15.725
8d	**90**	16.9±0.3	16.8±1.6	16.6±1.5	16.9±1.1	16.800
8e	**79**	32.5±0.2	32.1±0.1	32.4±0.2	32.9±0.6	32.474
9a	**92**	24.5±2.6	23.6±2.2	24.6±2.9	24.8±1.4	24.375
9b	**96**	22.3±2.5	22.9±1.8	22.5±2.3	22.2±1.4	22.475
9c	**89**	18.2±0.6	17.9±0.3	18.8±0.5	18.9±0.8	18.475
9d	**91**	29.4±3.6	28.5±2.8	32.6±3.5	29.2±8.2	29.925
9e	**89**	25.5±2.6	25.6±2.2	25.6±2.9	25.8±1.4	25.375
Doxorubicin	--	1.21 ± 0.80	0.90± 0.62	1.41 ± 0.58	1.01 ± 0.82	1.136

Table 4. Effects of compounds **5a-c** and doxorubicin on active Caspases 3, 8, 9 and Cytochrome C in MCF-7 breast cancer cell line.

Compound Number	Caspase-3		Caspase-8		Caspase-9		Cytochrome C	
	Conc (pg/ml)	Fold change	Conc (ng/ml)	Fold change	Conc (ng/ml)	Fold change	Conc (ng/ml)	Fold change
5a	388.58 ±4.20	5.92	0.93	5.47	12.83	13.79	0.548	11.91
5b	310.47 ±2.19	4.73	--	--	--	--	--	--
5c	345.92 ±3.92	5.27	--	--	--	--	--	--
Doxorubicin	503.20 ±4.22	7.66	1.75	10.07	16.23	17.40	0.604	13.13
Control	65.64	1	0.17	1	0.93	1	0.046	1

Table 5. Bax and Bcl-2 levels for compounds **5a**, **5b** and Doxorubicin in MCF-7 breast cancer cell line

Compound Number	Bax		Bcl-2	
	Conc (pg/ml)	Fold change	Conc (ng/ml)	Fold change
5a	241.30	29.21	1.085	4.68
5b	172.14	20.84	1.943	2.61
Doxorubicin	276.19	33.43	0.983	5.17
Cont.	8.26	1	5.086	1.00

Table 6: Molecular properties of compounds **5a-e** and **8a-c** predicted using Swiss ADME website.

MOLECULE	5a	5b	5c	5d	5e	8a	8b	8c
MW	405.83	391.81	419.86	426.25	484.73	429.86	415.83	429.86
#HEAVY ATOMS	29	28	30	29	30	31	30	31
#AROMATIC HEAVY ATOMS	16	16	16	16	16	25	25	25
FRACTION CSP3	0.14	0.1	0.17	0.1	0.14	0.13	0.09	0.13
#ROTATABLE BONDS	3	3	4	3	4	1	1	1
#H-BOND ACCEPTORS	5	5	5	5	5	5	5	5
#H-BOND DONORS	0	1	1	1	1	0	1	1
MR	111.58	106.68	116.46	111.69	119.19	117.8	112.9	117.86
TPSA	76.61	87.47	87.47	87.47	87.47	74.31	85.17	85.17
/LOGP	3.68	3.25	3.59	3.42	3.68	3.58	3.16	3.4
XLOGP3	3.42	3.24	3.97	3.86	4.29	3.76	3.58	3.94
WLOGP	4.13	4.12	4.81	4.77	5.27	4.22	4.21	4.52
MLOGP	2.69	2.48	2.9	2.96	3.28	3.99	3.78	3.99
SILICOS-IT LOG P	4.53	5.05	5.97	5.69	6.12	3.59	4.12	4.64
CONSENSUS LOG P	3.69	3.63	4.25	4.14	4.53	3.83	3.77	4.1
ESOL LOG S	-4.72	-4.54	-5.07	-5.12	-5.68	-5.4	-5.22	-5.52
ESOL SOLUBILITY (MG/ML)	7.71E-03	1.14E-02	3.53E-03	3.20E-03	1.02E-03	1.69E-03	2.48E-03	1.30E-03
ESOL SOLUBILITY (MOL/L)	1.90E-05	2.92E-05	8.42E-06	7.50E-06	2.10E-06	3.94E-06	5.97E-06	3.03E-06
ESOL CLASS	Moderately soluble	Moderately soluble	Moderately soluble	Moderately soluble	Moderately soluble	Moderately soluble	Moderately soluble	Moderately soluble
ALI LOG S	-4.71	-4.75	-5.51	-5.39	-5.84	-5.01	-5.05	-5.43
ALI SOLUBILITY (MG/ML)	7.93E-03	6.96E-03	1.30E-03	1.72E-03	7.01E-04	4.17E-03	3.67E-03	1.60E-03
ALI SOLUBILITY (MOL/L)	1.95E-05	1.78E-05	3.11E-06	4.04E-06	1.45E-06	9.69E-06	8.82E-06	3.73E-06
ALI CLASS	Moderately soluble	Moderately soluble	Moderately soluble	Moderately soluble	Moderately soluble	Moderately soluble	Moderately soluble	Moderately soluble
SILICOS-IT LOGSW	-6.84	-7.29	-8.05	-7.87	-8.45	-7.83	-8.28	-8.65
SILICOS-IT SOLUBILITY (MG/ML)	5.91E-05	2.02E-05	3.71E-06	5.72E-06	1.70E-06	6.40E-06	2.19E-06	9.56E-07
SILICOS-IT SOLUBILITY (MOL/L)	1.46E-07	5.16E-08	8.83E-09	1.34E-08	3.52E-09	1.49E-08	5.27E-09	2.22E-09
SILICOS-IT CLASS	Poorly soluble	Poorly soluble	Poorly soluble	Poorly soluble	Poorly soluble	Poorly soluble	Poorly soluble	Poorly soluble
GI ABSORPTION	High	High	High	High	High	High	High	High
BBB PERMEANT	No	No	No	No	No	Yes	No	No
PGP SUBSTRATE	No	No	No	No	No	Yes	Yes	Yes
CYP1A2 INHIBITOR	No	Yes	No	Yes	Yes	No	No	No
CYP2C19 INHIBITOR	Yes	Yes	Yes	Yes	Yes	Yes	Yes	Yes
CYP2C9 INHIBITOR	Yes	Yes	Yes	Yes	Yes	Yes	Yes	Yes
CYP2D6 INHIBITOR	No	No	No	No	No	No	No	No
CYP3A4 INHIBITOR	Yes	Yes	Yes	Yes	Yes	No	No	No
LOG K_P (CM/S)	-6.35	-6.39	-6.04	-6.16	-6.21	-6.25	-6.29	-6.12
LIPINSKI #VIOLATIONS	0	0	0	0	0	0	0	0
GHOSE #VIOLATIONS	0	0	0	0	1	0	0	0
VEBER #VIOLATIONS	0	0	0	0	0	0	0	0
EGAN #VIOLATIONS	0	0	0	0	0	0	0	0
MUEGGE #VIOLATIONS	0	0	0	0	0	0	0	0

BIOAVAILABILITY SCORE	0.55	0.55	0.55	0.55	0.55	0.55	0.55	0.55
PAINS #ALERTS	0	0	0	0	0	0	0	0
BRENK #ALERTS	2	2	2	2	2	0	0	0
LEADLIKENESS #VIOLATIONS	1	1	2	2	2	2	2	2
SYNTHETIC ACCESSIBILITY	4.15	4.08	4.29	4.08	4.19	3.86	3.75	3.86

Table 7: Molecular properties of compounds **8d,e** and **9a-e** predicted using Swiss ADME website.

MOLECULE	**8D**	**8E**	**9A**	**9B**	**9C**	**9D**	**9E**
MW	450.28	494.73	481.89	467.86	481.89	502.31	546.76
#HEAVY ATOMS	31	31	35	34	35	35	35
#AROMATIC HEAVY ATOMS	25	25	30	30	30	30	30
FRACTION CSP3	0.09	0.09	0.08	0.04	0.08	0.04	0.04
#ROTATABLE BONDS	1	1	2	2	2	2	2
#H-BOND ACCEPTORS	5	5	6	6	6	6	6
#H-BOND DONORS	1	1	0	1	1	1	1
MR	117.91	120.6	130.54	125.63	130.6	130.64	133.33
TPSA	85.17	85.17	87.45	98.31	98.31	98.31	98.31
ILOGP	3.38	3.49	3.88	3.56	3.78	3.76	3.89
XLOGP3	4.21	4.27	4.13	3.94	4.31	4.57	4.63
WLOGP	4.87	4.98	5.18	5.17	5.47	5.82	5.93
MLOGP	4.26	4.36	3.65	3.45	3.65	3.91	4.01
SILICOS-IT LOG P	4.76	4.79	3.97	4.5	5.02	5.13	5.17
CONSENSUS LOG P	4.29	4.38	4.16	4.12	4.45	4.64	4.73
ESOL LOG S	-5.81	-6.13	-5.93	-5.74	-6.05	-6.34	-6.65
ESOL SOLUBILITY (MG/ML)	6.90E-04	3.68E-04	5.64E-04	8.44E-04	4.34E-04	2.32E-04	1.23E-04
ESOL SOLUBILITY (MOL/L)	1.53E-06	7.44E-07	1.17E-06	1.80E-06	9.01E-07	4.62E-07	2.24E-07
ESOL CLASS	Moderately soluble	Poorly soluble	Moderately soluble	Moderately soluble	Poorly soluble	Poorly soluble	Poorly soluble
ALI LOG S	-5.71	-5.77	-5.67	-5.7	-6.09	-6.36	-6.42
ALI SOLUBILITY (MG/ML)	8.81E-04	8.39E-04	1.02E-03	9.24E-04	3.93E-04	2.20E-04	2.08E-04
ALI SOLUBILITY (MOL/L)	1.96E-06	1.70E-06	2.12E-06	1.98E-06	8.16E-07	4.39E-07	3.80E-07
ALI CLASS	Moderately soluble	Moderately soluble	Moderately soluble	Moderately soluble	Poorly soluble	Poorly soluble	Poorly soluble
SILICOS-IT LOGSW	-8.86	-9.05	-9.12	-9.57	-9.94	-10.15	-10.33
SILICOS-IT SOLUBILITY (MG/ML)	6.20E-07	4.41E-07	3.67E-07	1.26E-07	5.49E-08	3.56E-08	2.55E-08
SILICOS-IT SOLUBILITY (MOL/L)	1.38E-09	8.91E-10	7.62E-10	2.69E-10	1.14E-10	7.10E-11	4.66E-11
SILICOS-IT CLASS	Poorly soluble	Poorly soluble	Poorly soluble	Poorly soluble	Poorly soluble	Insoluble	Insoluble
GI ABSORPTION	High	High	High	High	High	High	Low
BBB PERMEANT	No	No	No	No	No	No	No
PGP SUBSTRATE	Yes	Yes	Yes	Yes	Yes	Yes	Yes
CYP1A2 INHIBITOR	No	No	No	No	No	No	No

CYP2C19 INHIBITOR	Yes	Yes	No	No	No	No	No
CYP2C9 INHIBITOR	Yes	Yes	Yes	No	No	No	No
CYP2D6 INHIBITOR	No	No	No	No	No	No	No
CYP3A4 INHIBITOR	No	No	No	No	No	No	No
LOG K_P (CM/S)	-6.06	-6.29	-6.31	-6.36	-6.18	-6.12	-6.35
LIPINSKI #VIOLATIONS	1	1	0	0	0	1	1
GHOSE #VIOLATIONS	0	1	2	0	2	3	3
VEBER #VIOLATIONS	0	0	0	0	0	0	0
EGAN #VIOLATIONS	0	0	0	0	0	0	0
MUEGGE #VIOLATIONS	0	0	0	0	0	0	0
BIOAVAILABILITY SCORE	0.55	0.55	0.55	0.55	0.55	0.55	0.55
PAINS #ALERTS	0	0	0	0	0	0	0
BRENK #ALERTS	0	0	0	0	0	0	0
LEAD LIKENESS #VIOLATIONS	2	2	2	2	2	2	2
SYNTHETIC ACCESSIBILITY	3.76	3.77	4.11	4	4.11	4	4.01

Graphical Abstract

Cell cycle arrest at G2/M phases

High oral absorption

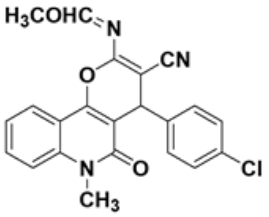

5a

Compound Number	Bax		Bcl-2	
	Conc (pg/ml)	Fold change	Conc (ng/ml)	Fold change
5a	241.30	29.21	1.085	4.68
Doxorubicin	276.19	33.43	0.983	5.17
Cont.	8.26	1	5.086	1.00

Compound Number	Caspase-3		Caspase-8		Caspase-9		Cytochrome C	
	Conc (pg/ml)	Fold change	Conc (ng/ml)	Fold change	Conc (ng/ml)	Fold change	Conc (ng/ml)	Fold change
5a	388.58 ±4.20	5.92	0.93	5.47	12.83	13.79	0.548	11.91
Doxorubicin	503.20 ±4.22	7.66	1.75	10.07	16.23	17.40	0.604	13.13
Control	65.64	1	0.17	1	0.93	1	0.046	1

Highlights

A series of pyrano[3,2-c]quinoline/triazolopyrimidine hybrids was made.

Products were characterized by IR, MS, and multinuclear NMR (^{1}H, ^{13}C, and ^{15}N).

The products showed antiproliferative activity versus cancer cell lines.

Open chain formimidic esters were more potent than heteroannulated systems.

The most active compounds were also studied for caspase activation.

Conflicts of interest

The authors declare no conflict of interest